ECONSTOR
Make Your Publications Visible.

A Service of

ZBW Leibniz-Informationszentrum Wirtschaft
Leibniz Information Centre for Economics

Heinrich, Markus

Working Paper

Does the Current State of the Business Cycle matter for Real-Time Forecasting? A Mixed-Frequency Threshold VAR approach.

Suggested Citation: Heinrich, Markus (2020) : Does the Current State of the Business Cycle matter for Real-Time Forecasting? A Mixed-Frequency Threshold VAR approach., ZBW – Leibniz Information Centre for Economics, Kiel, Hamburg

This Version is available at:
https://hdl.handle.net/10419/219312

Standard-Nutzungsbedingungen:

Die Dokumente auf EconStor dürfen zu eigenen wissenschaftlichen Zwecken und zum Privatgebrauch gespeichert und kopiert werden.

Sie dürfen die Dokumente nicht für öffentliche oder kommerzielle Zwecke vervielfältigen, öffentlich ausstellen, öffentlich zugänglich machen, vertreiben oder anderweitig nutzen.

Sofern die Verfasser die Dokumente unter Open-Content-Lizenzen (insbesondere CC-Lizenzen) zur Verfügung gestellt haben sollten, gelten abweichend von diesen Nutzungsbedingungen die in der dort genannten Lizenz gewährten Nutzungsrechte.

Terms of use:

Documents in EconStor may be saved and copied for your personal and scholarly purposes.

You are not to copy documents for public or commercial purposes, to exhibit the documents publicly, to make them publicly available on the internet, or to distribute or otherwise use the documents in public.

If the documents have been made available under an Open Content Licence (especially Creative Commons Licences), you may exercise further usage rights as specified in the indicated licence.

WWW.ECONSTOR.EU

Mitglied der Leibniz-Gemeinschaft

Does the Current State of the Business Cycle matter for Real-Time Forecasting? A Mixed-Frequency Threshold VAR approach.

Markus Heinrich*

University of Kiel

11th June 2020

Abstract

Macroeconomic forecasting in recessions is not easy due to the inherent asymmetry of business cycle phases and the increased uncertainty about the future path of the teetering economy. I propose a mixed-frequency threshold vector autoregressive model with common stochastic volatility in mean (MF-T-CSVM-VAR) that enables to condition on the current state of the business cycle and to account for time-varying macroeconomic uncertainty in form of common stochastic volatility in a mixed-frequency setting. A real-time forecasting experiment highlights the advantage of including the threshold feature for the asymmetry as well as the common stochastic volatility in mean in MF-VARs of different size for US GDP, inflation and unemployment. The novel mixed-frequency threshold model delivers better forecasts for short-term point and density forecasts with respect to GDP and unemployment– particularly evident for nowcasts during recessions. In fact, it delivers a better nowcast than the US Survey of Professional Forecasters for the sharp drop in GDP during the Great Recession in 2008Q4.

Keywords: Threshold VAR, Stochastic Volatility, Forecasting, Mixed-frequency Models, Business Cycle, Bayesian Methods

JEL-Codes: C11, C32, C34, C53, E32

*University of Kiel, Institute for Statistics and Econometrics, Olshausenstr. 40–60, 24118 Kiel, Germany, m.heinrich@stat-econ.uni-kiel.de

1 Introduction

Central banks, government agencies and the private sector turn to economic forecasts to gauge the current economic situation and future economic outlook. Having access to precise forecasts is crucial as a basis of decision-making. Making the right decision is particularly important in an uncertain and deteriorating economic environment, i.e. during the onset of a recession. Though, forecasts made at the beginning of recessions tend to err. Dovern and Jannsen (2017) uncover large systematic negative forecast errors made by professional forecasters for GDP growth during recessions. Chauvet and Potter (2013) reveal that forecasting GDP growth is generally more difficult in recessions than in expansions. In this paper I consider two potential reasons for these failures: First, insufficient good use of information about the current state of the business cycle in real-time. Second, missing information about early business cycle indicators at a higher frequency than the variable to be predicted. The main contribution of this paper is to combine those two features into one novel model. Therefore, I set up a mixed-frequency threshold VAR with common stochastic volatility in mean (MF-T-CSVM-VAR) that simultaneously identifies the current state of the business cycle in real-time and incorporates data with different frequencies.

Besides the significant benefits of mixed-frequency (MF) models that bear in mind frequency mismatches for forecasting, i.e. monthly indicators and quarterly GDP (see, i.e., Schorfheide and Song, 2015), a successful forecasting model needs to account for three well-documented business cycle characteristics. First, the business cylce can be characterized by the asymmetric dynamics in expansions and recessions. I model this asymmetry using the threshold feature by means of two distinct regimes within the VAR framework (T-VAR). This nonlinear VAR framework takes into account the nature of state dependent shock transmissions (see, i.e, Auerbach and Gorodnichenko, 2012; Caggiano et al., 2014; Mumtaz and Surico, 2015; Tenreyro and Thwaites, 2016). Second, business cycles can be characterized by co-movements among a broad range of different macroeconomic variables. Hence, I include a comprehensive business cycle index composed of a large data set as a predictor and threshold variable to identify the business cycle regimes in the T-VAR. And third, the business cycle often shares an increase (decrease) in macroeconomic uncertainty during recessions (expansions) as shown by, among others, Jurado et al. (2015). Clark (2011) and Clark and Ravazzolo (2015) point out the importance of time-varying volatilities for precise forecasts to account for changing uncertainty. On that account, I apply the concept of common stochastic volatility (CSV) as in Carriero et al. (2016) to account for the change in macroeconomic uncertainty over time. I add common stochastic volatility in the mean equation (CSVM) of the VAR as uncertainty can endogenously impact macroeconomic variables (see, i.e., Bloom, 2014; Carriero et al., 2018) and hence, can be beneficial for forecasting.

I stress the importance of considering these features of the business cycle for small and medium-scale MF-VARs in a real-time forecasting experiment on US GDP, inflation (CPI) and unemployment rate (UR). Overall, the nonlinear small-scale MF-T-VAR and MF-T-CSVM-VAR outperform their linear competitors on average across all variables and horizons. The best results are with regard to GDP and unemployment during recessions. The largest gains in relative forecast accuracy are during the steepest contraction in 2008Q4 during the Great Recession in which the MF-T-VAR even outperforms the GDP nowcast from the Survey of Professional

Forecasters (SPF). The medium-scale MF-CSVM-VAR performs best for forecast horizons two to four quarters ahead in which case it is quite competitive vis-á-vis the SPF for GDP. Accouting for macroeconomic uncertainty in form of CSVM generally contributes the most to density forecasts for all models and specifically to UR forecasts during recessions for small-scale models.

The novel fully-fledged MF-T-CSVM-VAR is based upon three extensions to the VAR which makes it flexible by switching on and off each feature as required. First is the MF-VAR in state-space form as in Schorfheide and Song (2015) to cope with unobserved low-frequency variables in mixed-frequency data.[1] Second is the T-VAR based on the Bayesian estimation algorithm proposed by Chen and Lee (1995). And third is the CSV based on Carriero et al. (2016) which additionally enters the mean equation as in Mumtaz and Theodoridis (2018). I utilize a Gibbs sampler to draw from each conditional posterior. Since VARs can suffer quite quickly from over-parameterization and overfitting, I apply shrinkage in form of a Minnesota Prior first proposed by Litterman (1986). I implement a flexible adaptive inverse-Gamma hyperprior on the overall and cross-variable shrinkage parameters. In case of regime dependent parameters, this prior setup allows for distinct shrinkage across regimes.

This paper adds to the literature on nonlinear forecast models in real-time with a particular focus on mixed-frequency, the state of the business cycle, macroeconomic uncertainty and threshold VARs.[2] Alessandri and Mumtaz (2017) reveal a good forecasting performance of a T-VAR with financial condition regimes during the Financial Crisis 2008-2009. Reif (2020) shows improved forecasts with a T-VAR that includes a macroeconomic uncertainty index and conditions on periods of high and low uncertainty. Furthermore, Segnon et al. (2018) illustrate the importance of uncertainty on forecasting US GNP growth whereas Pierdzioch and Gupta (2019) highlight the predictive power of uncertainty on forecasting US recessions. In terms of informative content of the state of the business cycle, Chauvet and Potter (2013) and Carstensen et al. (2020) report an improved forecasting performance for AR models in recessions for horizons up to 2 quarters ahead that incorporate a business cycle factor and recession probabilities as predictors for US and German GDP, respectively. With regard to mixed-frequency and business cycle regimes, Bessec and Bouabdallah (2015) and Barsoum and Stankiewicz (2015) use univariate Markov-Switching models to account for the business cycle pattern in a mixed-frequency approach. They show that these models can accurately date the business cycle and forecast US GDP growth. Carriero et al. (2015b) reveal the benefits of stochastic volatility for forecasting in a mixed-frequency setup. Most closely related to my study in terms of nonlinear multivariate mixed-frequency models is the paper by Foroni et al. (2015).[3] They apply a Markov-Switching mixed-frequency bi-variate VAR for improved GDP forecasts. Yet, none of the contributions so far combine all of these beneficial features into one comprehensive model.

The remainder of the paper is structured as follows: Section 2 depicts the competing models and explains the estimation methodology. Section 3 provides a description of the data set and outlines the forecast setup. Section 4 presents the empirical results and Section 5 concludes.

[1] Foroni and Marcellino (2013) offer a detailed survey on different mixed-frequency methods.

[2] D'Agostino et al. (2013), Barnett et al. (2014), Ferrara et al. (2015) and Aastveit et al. (2017), among others, provide comprehensive comparisons of different non-linear against linear models following the Great Recession.

[3] Götz and Hauzenberger (2018) and Heinrich and Reif (2020) combine mixed-frequency and time-varying parameter VARs, though this does not isolate the impact of the current state of the business cycle on forecasting.

2 Models

All models are estimated with Bayesian methods and can be written in state space form. The first subsection introduces the mixed-frequency (MF) block as the measurement equation which is necessary for all models. Subsequently, I present the different transition equations depending on the respective model. I start with the baseline MF-VAR followed by the common stochastic volatility in mean (CSVM). Finally, I extend the MF-VAR to the threshold VAR (MF-T-VAR) with and without CSVM. Thereafter, I describe the estimation algorithm and prior specifications.

2.1 Mixed-Frequency

The mixed-frequency block closely follows Schorfheide and Song (2015). Let y_t denote an $n \times 1$ vector of observable variables at monthly frequency t which is linked to the latent state vector z_t via the transformation matrix R_t:

$$y_t = R_t z_t \tag{1}$$

where the vector of variables is decomposed into $y_t = [y'_{q,t}, y'_{m,t}]'$ with n_q quarterly and n_m monthly variables. This vector contains missing values due to missing intra-quarterly values for $y_{q,t}$. Thus, a vector for one quarter is $[y_t \; y_{t-1} \; y_{t-2}]' = [[y'_{q,t}, y'_{m,t}]' \; [NaN', y'_{m,t-1}]' \; [NaN', y'_{m,t-2}]']'$ with missing values in month $t-1$ and $t-2$ of each quarter. The state vector includes p lags for the VAR. Hence, $z_t = [z'_{q,t}, z'_{m,t}]'$ is an $n(p+1) \times 1$ vector where $z_{q,t} = [\tilde{y}'_{q,t}, \ldots, \tilde{y}'_{q,t-p}]'$ is the unobserved quarterly variable at monthly frequency. $z_{m,t} = [y'_{m,t}, \ldots, y'_{m,t-p}]'$ is the vector of observed monthly variables.

The transformation from quarterly to monthly frequency is done according to a geometric mean of quarterly variables in levels $Y_{q,t}$ as in Mariano and Murasawa (2003):

$$Y_{q,t} = (\tilde{Y}_{q,t}\tilde{Y}_{q,t-1}\tilde{Y}_{q,t-2})^{1/3} \tag{2}$$

$$\Delta_3 \, ln(Y_{q,t}) = y_{q,t} = (1/3\,\tilde{y}_{q,t} + 2/3\,\tilde{y}_{q,t-1} + \tilde{y}_{q,t-2} + 2/3\,\tilde{y}_{q,t-3} + 1/3\,\tilde{y}_{q,t-4}). \tag{3}$$

where the lower case denotes growth rates. R_t is a time-varying transformation matrix:

$$R_t = \begin{bmatrix} R_{1,t} & R_{2,t} \end{bmatrix}' \tag{4}$$

$$R_{1,t} = \begin{bmatrix} 1/3 * I_{nq} & 0_{nq \times n-1} & 2/3 * I_{nq} & 0_{nq \times n-1} & I_{nq} & 0_{nq \times n-1} & 2/3 * I_{nq} & 0_{nq \times n-1} & \ldots \\ & 1/3 * I_{nq} & 0_{nq \times n-1} & 0_{nq \times (p-4)n} \end{bmatrix} \tag{5}$$

$$R_{2,t} = \begin{bmatrix} 0_{n-nq \times 1} & I_{n-nq} & 0_{n-nq \times pn} \end{bmatrix}. \tag{6}$$

The time variation in R_t follows Durbin and Koopman (2001) to deal with missing observations in y_t. If a variable is not observed at time t, the respective row in equation (1) is deleted and thus skipped in the respective estimation step of the Kalman filter.

2.2 Mixed-Frequency VAR

Conditional on the latent $\tilde{y}_{q,t}$, the $n \times 1$ vector $\tilde{y}_t = [\tilde{y}'_{q,t}, y'_{m,t}]'$ is modeled as a standard VAR with p lags, constant parameters and homoscedasticity:

$$\tilde{y}_t = A_0 + \sum_{l=1}^{p} A_l \tilde{y}_{t-l} + u_t \qquad\qquad u_t \sim \mathcal{N}(0, \Omega) \tag{7}$$

where A_0 is an $n \times 1$ vector of intercepts, A_l is $n \times n$ matrix of coefficients for $l = 1, \ldots, p$ and u_t denotes the $n \times 1$ error vector with a constant variance-covariance matrix Ω. The VAR(p) can be rewritten as a VAR(1) and completes the state space model with equation (1) for the MF-VAR:

$$z_t = C + A z_{t-1} + \upsilon_t \qquad\qquad \upsilon_t \sim \mathcal{N}(0, \Xi) \tag{8}$$

where $z_t = [\tilde{y}'_t, \ldots, \tilde{y}'_{t-p}]'$. C and A contain A_0 and $A_1, \ldots A_p$, respectively, in the first n rows for the VAR dynamics. Ξ contains Ω in the first n rows for the variance-covariance matrix.

2.3 Common Stochastic Volatility in Mean

Common Stochastic Volatility (CSV) is based on Carriero et al. (2016). They exploit the finding that stochastic volatilities of different variables often share a comparable pattern and thus, a single volatility factor is sufficient to capture the bulk of time variation in volatility. I extract a common factor f_t with loadings all restricted to one by decomposing the variance-covariance matrix of the error vector $u_t \sim \mathcal{N}(0, f_t \Sigma)$ from equation (7). The matrix Σ captures the difference in scaling among the variables and f_t accounts for the time-variation resulting in a time-varying variance-covariance matrix $\Omega_t = f_t \Sigma$.

This concept can be further enhanced by implementing CSV in the mean equation of the VAR (CSVM) :

$$\tilde{y}_t = A_0 + \sum_{l=1}^{p} A_l \tilde{y}_{t-l} + b h_{t-1} + \Sigma^{1/2} f_t^{1/2} \epsilon_t \qquad\qquad \epsilon_t \sim \mathcal{N}(0, I) \tag{9}$$

where $h_{t-1} = ln(f_{t-1})$ is the log volatility and $\Sigma^{1/2}$ is a lower triangular matrix such that $Var(u_t | f_t) = (\Sigma^{1/2} f_t^{1/2})(\Sigma^{1/2} f_t^{1/2})' = f_t \Sigma = \Omega_t$. h_t follows a random walk law of motion:

$$h_t = h_{t-1} + \varsigma_t \qquad\qquad \varsigma_t \sim \mathcal{N}(0, \phi) \tag{10}$$

which is, on the one hand, a parsimonious specification and on the other hand, as shown by Clark and Ravazzolo (2015), comparable in forecast accuracy to other specifications.

2.4 Mixed-frequency Threshold VAR

The mixed-frequency Threshold VAR (MF-T-VAR) separates the linear VAR into different regimes, which in my case are expansions and recessions. The regimes are identified by a threshold variable y^*_{t-d} in form of a monthly business cycle index from the observed monthly vector

$y_{m,t}$, the delay parameter d and the respective threshold value r such that the VAR dynamics are modeled as follows:

$$\tilde{y}_t = A_{0,S_t} + \sum_{l=1}^{p} A_{l,S_t}\tilde{y}_{t-l} + \Sigma_{S_t}^{1/2}\epsilon_t \qquad \epsilon_t \sim \mathcal{N}(0, I) \tag{11}$$

$$\text{with } S_t = \begin{cases} 1 & \text{if } y^*_{t-d} \leq r \\ 2 & \text{otherwise.} \end{cases} \tag{12}$$

This model allows for different VAR coefficients $A_{0,S_t}, \ldots, A_{p,S_t}$ and variance-covariance matrix $Var(u_t) = \Sigma_{S_t}^{1/2}(\Sigma_{S_t}^{1/2})' = \Omega_{S_t}$ across regimes.

Furthermore, I extend the MF-T-VAR with common stochastic volatility in mean (MF-T-CSVM-VAR) such that equation (11) changes to:

$$\tilde{y}_t = A_{0,S_t} + \sum_{l=1}^{p} A_{l,S_t}\tilde{y}_{t-l} + b_{S_t}h_{t-1} + \Sigma_{S_t}^{1/2} f_t^{1/2}\epsilon_t \qquad \epsilon_t \sim \mathcal{N}(0, I) \tag{13}$$

and hence, $Var(u_t|f_t) = (\Sigma_{S_t}^{1/2} f_t^{1/2})(\Sigma_{S_t}^{1/2} f_t^{1/2})' = f_t\Sigma_{S_t} = \Omega_{t,S_t}$. On the one hand, the matrix Σ_{S_t} allows for different scalings across the regimes. On the other hand, the factor f_t grants time variation within the regime and permits feedback through the mean equation. Again, the law of motion for h_t follows a random walk as in equation (10).

Together with the measurement equation (1), the MF-T-CSVM-VAR(p) can be written down as a MF-T-CSVM-VAR(1) in state space form:

$$z_t = C_{S_t} + A_{S_t}z_{t-1} + B_{S_t}h_{t-1} + \upsilon_t \qquad \upsilon_t \sim \mathcal{N}(0, \Xi_{t,S_t}). \tag{14}$$

where $z_t = [\tilde{y}_t', \ldots, \tilde{y}_{t-p}']'$. C_{S_t} and A_{S_t} contain A_{0,S_t} and $A_{1,S_t}, \ldots A_{p,S_t}$, respectively, in the first n rows for the VAR dynamics. B_{S_t} contains b_{S_t} in the first n rows for the CSVM part. Ξ_{t,S_t} contains Ω_{t,S_t} in the first n rows for the time-varying variance-covariance matrix. A detailed description of the state space form of the MF-T-CSVM-VAR is in Appendix A.

2.5 Prior Specification and Estimation

I estimate all VARs with an independent Normal-inverse-Wishart prior and impose Minnesota shrinkage on the VAR coefficients. This prior setup is more flexible compared to the dependent Normal-inverse-Wishart prior since the independence allows for cross-variable shrinkage in the variance component of the Normal prior amplifying forecast accuracy (see Carriero et al., 2015a). The prior mean on the first lag is 0 (0.9) if the respective variable is non-persistent (persistent) since all variables are transformed to be stationary (see Karlsson, 2013, for variations on the Minnesota prior). The prior variance for row j and column i of the coefficient matrix of lag l is set as follows:

$$Var(A_l^{j,i}) = \begin{cases} \frac{\lambda_1}{l^2} & \text{if } i = j \\ \frac{\lambda_1 \lambda_2 \sigma_{jj}^2}{l^2 \sigma_{ii}^2} & \text{if } i \neq j \\ \frac{\lambda_1 \lambda_3 \sigma_{jj}^2}{l^2 \sigma_{ii}^2} & \text{if } i \neq j \wedge j = y^* \\ 1000 & \text{if } l = 0 \end{cases} \tag{15}$$

where σ_{ii} is the residual standard error of an AR(p) for variable i. The amount of shrinkage is determined by the vector of hyperparameters $\Lambda = [\lambda_1, \lambda_2, \lambda_3]'$. λ_1 governs the overall and λ_2 the cross-variable shrinkage. Hence, it is assumed that lags on other variables contain less information compared to own lags if $\lambda_2 < 1$. Though, since the main concept of this paper is build around the importance of the business cycle, I apriori assume a stronger influence from the business cycle variables, namely the monthly BC index y^* and the log of the volatility factor h_t. Hence, I add λ_3 as an extra shrinkage parameter (denoted as BC shrinkage hereafter).[4] I facilitate regime-dependent shrinkage for the T-VARs to examine whether shrinkage is different in recessions and expansions, thus Λ is different across regimes Λ_{S_t} for $S_t = 1, 2$. The vector of shrinkage parameters is estimated using an inverse-Gamma hyperprior:[5]

$$p(\lambda_i) \sim \mathcal{IG}(\alpha, \beta_i) \qquad\qquad i = 1, 2, 3$$

with shape $\alpha = 0.1$ and scale $\beta_i = 0.044$ for $i = 1, 2$ and scale $\beta_i = \sqrt{0.044}$ for $i = 3$ chosen such that it is weakly informative and has a mode of 0.04 for $i = 1, 2$, which is in line with common values used for US data, and a mode of 0.2 which assigns apriori less shrinkage for the business cycle variables.[6]

The prior scale matrix for the inverse-Wishart is diagonal where the diagonal elements are the residual variances of ARs(p). The degrees of freedom are set to a minimum $n+2$ to resemble a rather loose prior. I follow Carriero et al. (2016) for the CSV by using an inverse-Gamma prior for the variance ϕ with mean 0.01 and scale 4. The stochastic volatility factor f_t has a Normal prior with mean 1 and variance 0.5. I fix $f_0 = 1$ for identification. I assume a uniform prior for the delay parameter $d \sim \mathcal{U}(1, p)$ as well as for the threshold parameter $r \sim \mathcal{U}(y_q^*, y_{1-q}^*)$, where $q = 0.10$ denotes the quantile of the threshold variable to avoid identification of outlier regimes instead of business cycle regimes. Further details on prior and initial values are given in Appendix B.

I estimate the fully-fledged MF-T-CSVM-VAR with a Metropolis-within-Gibbs sampler. All the remainder models can be estimated by simply turning off the respective step within the

[4] A comparison between the standard cross-variable shrinkage $\lambda_3 == \lambda_2$ and the BC shrinkage $\lambda_3 \neq \lambda_2$ with respect to their point forecast accuracy is in Appendix E.

[5] The concept of the Normal-inverse-Gamma mixture prior follows the idea of Geweke (1993) who shows that if $\alpha = \beta$, this is equivalent to a Student-t prior (see also Korobilis, 2013).

[6] See, e.g., Alessandri and Mumtaz (2017) for a T-VAR with overall shrinkage λ_1 and Carriero et al. (2015a) for the same value for cross-variable shrinkage λ_2. The mode of λ_3 is 5 times larger than the mode of λ_1 and λ_2 due to the importance of the monthly BC index for estimating the latent monthly GDP. The value approximately resembles the strong correlation between the BC index and GDP at quarterly frequency. This correlation is, depending on the data vintage, between 4 and 5.5 times larger than the second highest correlation for GDP.

sampler. The conditional MF part is estimated along the lines of Schorfheide and Song (2015) with a Kalman filter. The conditional T-VAR is based on Chen and Lee (1995). Hence, r is drawn with a random walk Metropolis-Hastings. The prior for λ_i is natural conjugate for the conditional posterior distribution and thus, follows an inverse-Gamma distribution. The draws for the stochastic volatility are carried out with the algorithm of Jacquier et al. (2002).[7] The MCMC sampler has 30000 draws. The first 25000 are burn-in draws while the last 5000 draws are for inference. The lag length is set to $p = 6$ as in Schorfheide and Song (2015). A detailed description of the sampler is in Appendix C.

2.6 Now- and Forecasting Density

The predictive densities are simulated within the MCMC sampler. Let T denote the size of the respective real-time data vintage. Since real-time data contains ragged edges due to publication lags, the Kalman filter fills in missing values at the end of each vintage up to T. I apply iterated multistep forecasts $\tilde{y}_{T+h_m}$ for the remaining monthly forecast horizons $h_m = 1, \dots, 12$, which are drawn at iteration s of the MCMC sampler for the MF-T-CSVM-VAR from:

$$p(\tilde{y}^{(s)}_{T+h_m} | \tilde{y}^{(s)}_{1:T+h_m-1}, \theta^{(s)}_{S_{T+h_m}}) \\ \sim \mathcal{N}(C^{(s)}_{S_{T+h_m}} + A^{(s)}_{S_{T+h_m}} \tilde{y}^{(s)}_{(T+h_m-p:T+h_m-1)} + b^{(s)}_{1,S_{T+h_m}} h^{(s)}_{T+h_m-1}, \Omega^{(s)}_{T+h_m,S_{T+h_m}}) \quad (16)$$

where $\tilde{y}_{1:T} = [\tilde{y}_1, \dots, \tilde{y}_T]'$ and θ contains all remaining parameters of the model. For both T-VARs, the first forecast is conditional on the state S_t at time T and evolves according to equation (12) with respect to the threshold value $r^{(s)}$. I draw a sequence of $f^{(s)}_{T+h_m}$ common volatility factors for $h_m = 1, \dots, 12$ according to the random walk law of motion as in equation (10) to forecast the time varying volatilities $\Omega^{(s)}_{T+h_m,S_{T+h_m}} = f^{(s)}_{T+h_m} \Sigma^{(s)}_{S_{T+h_m}}$.

3 Data and Forecast Setup

3.1 Data Setup

The data set includes US real-time data covering March 1967 until December 2017 from the Archival FRED database and the FRED-MD monthly database provided by McCracken and Ng (2016). The historical vintages start in February 2001 up to December 2017. This provides a total of 203 vintages including the 2001 and 2008/09 recession for the real-time forecasting experiment. The target variables to be forecasted are Real Gross Domestic Product (GDP), the Unemployment Rate (UR) and the Consumer Price Index (CPI).

I distinguish between two variable sets with respect to size–a small-scale and a medium-scale set. Since GDP is in quarterly frequency, the small-scale set requires a monthly business cycle index to accurately estimate the intra-quarterly values of GDP. Here I distinguish between two indices. As a benchmark index, I choose Industrial Production (IP) as it is generally considered

[7] This algorithm draws f_t date by date for $t = 1, \dots, T$ instead of in one block as in Kim et al. (1998). Hence, it can accommodate the stochastic volatility in mean.

to be good predictor for GDP (see, i.e., Foroni et al., 2015; Brave and Butters, 2010). Since the business cycle is characterized by co-movements among a broad range of different macroeconomic variables, I utilize the Chicago Fed National Activity Index (CFNAI) as a more comprehensive business cycle index. The index is based on the first principle component from a data set containing 85 monthly macroeconomic variables. I choose this index for three reasons. First, the index allows for accurately classifying the economy into recessions and expansions (see, i.e., Berge and Jorda, 2011; Brave, 2009) and hence, can be used as a threshold variable in equation (12). Second, it is good for nowcasting GDP (see Brave and Butters, 2014). And third, it starts quite early in March 1967, is in monthly frequency and the real-time data vintages are publicly available since February 2001. As the index neither cover interest rates nor stock market data, I additionally include in both small-scale sets the yield spread (YS), measured as the difference between the 10-year and the 3-month treasury bill rate, and the S&P 500 index. Both variables are good predictors for the business cycle (see, i.e., Chauvet and Potter, 2005; Liu and Moench, 2016) as well as for the target variables (see, i.e., Estrella and Mishkin, 1997; Estrella, 2005; Evgenidis et al., 2020). Hence, the two small-scale sets include GDP, CPI, UR, YS, S&P 500 and IP or CFNAI as a business cycle index.

The medium scale set is based on the evidence in the literature that medium-scale VARs in many cases outperform small-scale VARs (see, i.e., Bańbura et al., 2010; Koop, 2013). Carriero et al. (2019) shown that large-scale VARs in many cases do not outperform medium-scale VARs with 13-14 hand-picked variables. Hence, I append the small-scale set with two important variables from each of the four categories of the CFNAI–namely, 1) production and income, 2) labour market, 3) personal consumption and housing and 4) sales, orders and inventories–in exchange for the CFNAI.[8] This provides me with 13 variables for the medium-scale set and allows to analyse whether the CFNAI index alone or the individual variables are crucial for precise forecasts. These variables are Industrial Production, Capacity Utilization, Average Weekly Hours, All Employees-Total Nonfarm, Housing Starts, Real Personal Consumption Expenditures, Real Manufacturing and Trade Sales and New Orders Durable Goods. This variable set is quite standard for medium-scale VARs for US data and is similar to data sets of other US studies (see, i.e., Schorfheide and Song, 2015; Carriero et al., 2016, 2019).

All variables are transformed to be stationary. The CFNAI is taken as a real-time three month moving average to filter out some of the volatility since it is shown to better reflect the business cycle. Table 1 provides a quick overview about the included variables in each set. A full list of all variables with the respective transformation and source is in Appendix F.

[8]The importance is measured in terms of factor loadings in the principle component analysis. Furthermore, the choice is also based on availability in real-time over the time span February 2001 - December 2017. A full list of all monthly indicators and their loadings can be found here: https://www.chicagofed.org/~/media/publications/cfnai/background/cfnai-background-pdf.pdf.

Table 1: Sets of Variables

	Small Benchmark^b	Small	Medium^{med}
GDP	x	x	x
CPI	x	x	x
Unemployment Rate	x	x	x
Yield Spread	x	x	x
S&P 500	x	x	x
CFNAI		x	
Industrial Production	x		x
Capacity Utilization			x
Average Weekly Hours			x
Employment			x
Housing Starts			x
Consumption			x
Manufacturing & Trade Sales			x
New Orders Durable Goods			x

Notes: For the remainder, a model M with a medium variable set is denoted by M^{med} and the benchmark model with M^b. A list of the data with source and transformation can be found in Appendix F.

Combining the data sets with the different models described in Section 2, I analyse a total of seven models for the forecasting experiment:[9]

1. MF-VAR^b: Mixed-frequency VAR (small benchmark)
2. MF-VAR: Mixed-frequency VAR (small)
3. MF-CSVM-VAR: Mixed-frequency VAR with common stochastic volatility in mean (small)
4. MF-T-VAR: Mixed-frequency threshold VAR (small)
5. MF-T-CSVM-VAR: Mixed-frequency threshold VAR with common stochastic volatility in mean (small)
6. MF-VAR^{med}: Mixed-frequency VAR (medium)
7. MF-CSVM-VAR^{med}: Mixed-frequency VAR with common stochastic volatility in mean (medium)

3.2 Forecast Setup

I apply an expanding window to the 203 real-time data vintages from February 2001 until December 2017. Since GDP is in quarterly frequency, all forecasts are evaluated at $h = 1, \ldots, 4$ quarters

[9] Due to the nonlinearity, T-VARs become quite tedious and time-consuming to estimate with increasing scale. Hence, I do not include medium-scale T-VARs.

ahead which relates to the quarterly averages of monthly forecast $h_m = 1, \ldots, 12$. Monthly GDP is taken in quarterly growth rates via the transformation matrix R_t in equation (4). Hence, in the end I obtain quarterly averages of monthly GDP in quarterly growth rates, quarterly averages of monthly CPI inflation and quarterly averages of monthly unemployment rates as final forecast values.

The timing and availability of the data is vital since forecasts are made in real-time. I assume that forecasts are made at the end of each month as the CFNAI is published in the last week of the month and is crucial for the estimation of the threshold VAR. The forecaster has only the information at its disposal as in real-time. Thus, the data set includes so called "ragged edges" due to publication lags and data revisions. Only the yield spread and the S&P 500 are available without a lag. All other variables have a publication lag according to the ALFRED and Fred MD real-time data base.

The timing is crucial for $h = 1$ which constitutes a nowcast as it refers to the quarter in which the forecast is made. Lets take for example the real-time data vintage 2008M2 for nowcasting 2008Q1. The publication lags at the end of the vintage for January to February 2008 are filled with forecasts by the Kalman Filter, while the forecast for March 2008 is simulated by equation (16) for $h_m = 1$. Thus, the quarterly nowcast $h = 1$ is an average of January, February and March, where January and February are from the Kalman Filter and March from forecast $h_m = 1$.

4 Results

This section starts with a brief presentation of the in-sample and out-of-sample results concerning the regime identification of the MF-T-CSVM-VAR.[10] Next, I show in-sample results with respect to shrinkage and common stochastic volatility. After that, I present the results from the out-of-sample forecasting experiment. The forecast accuracy is evaluated with respect to point and density forecasts and conditional on recession and expansion subsamples. Furthermore, I compare the nowcast accuracy against the Survey of Professional Forecasters with a special focus on the Great Recession.

4.1 Regimes

The important feature of T-VARs is the ability to separate samples into different regimes in a data driven manner defined by the threshold variable. Figure 1a depicts the Chicago Fed National Activity Index along with the estimated threshold r and the regime $S_t = 1$ for the final data vintage 1967M4-2017M12. The state $S_t = 1$ clearly identifies a recession regime as it closely matches the NBER recessions. Furthermore, the threshold value of -0.59 is similar to the one found in Berge and Jorda (2011) with -0.72 and thus confirms the good ability of the CFNAI for classifying economic activity into recessions and expansions.

Since the CFNAI includes monthly economic indicators, which are prone to revisions, Figure 1b displays the real-time out-of-sample nowcast results for the regimes together with the time varying threshold value r over the expanding recursive out-of-sample 2001M2-2017M12. The

[10] Results for the MF-T-VAR are quantitatively similar and available upon request.

threshold value is quite stable over time. It starts at roughly -0.7 and remains around that value in the first part of the out-of-sample period. After that, it increased slightly to approximately -0.6 right after the Great Recession in 2009. Overall, the real-time estimates significantly differ to the final estimates only in three occasions–the beginning and the end of the Great Recession and the 2008M8 vintage. These differences are due to revisions. The onset of the Great Recession as well as the short recovery in 2008M8 have been revised downwards quite heavily at a later vintage. Furthermore, the Great Recession regime prevails 6 month longer out-of-sample compared to only 2 month longer in-sample. Again, this is evident in data revisions as the index has been revised upwards at a later stage. In summary, the CFNAI is able to accurately and timely date the business cycle in-sample and out-of-sample.

Figure 1: Chicago Fed National Activity Index and Threshold Regimes

(a) In-sample

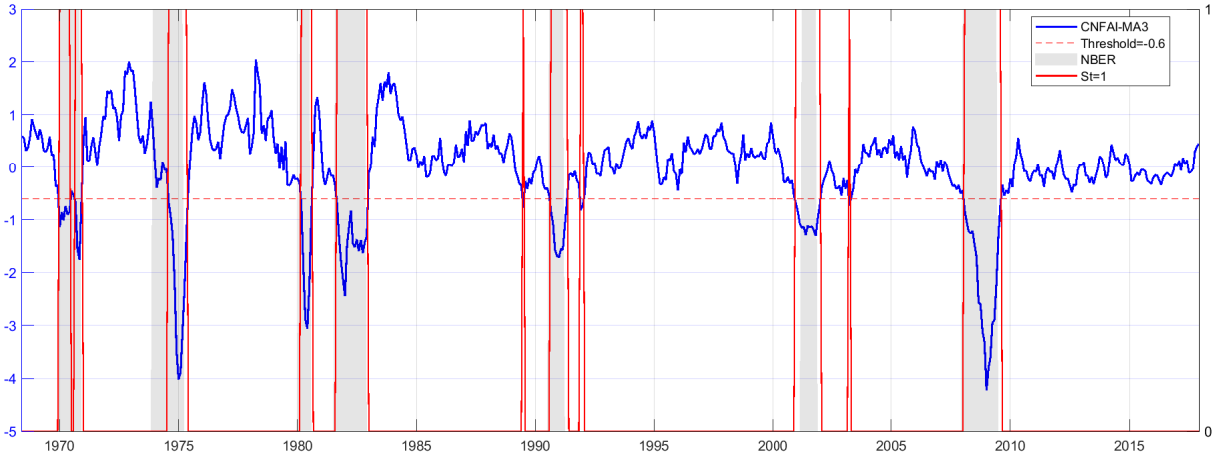

(b) Out-of-sample

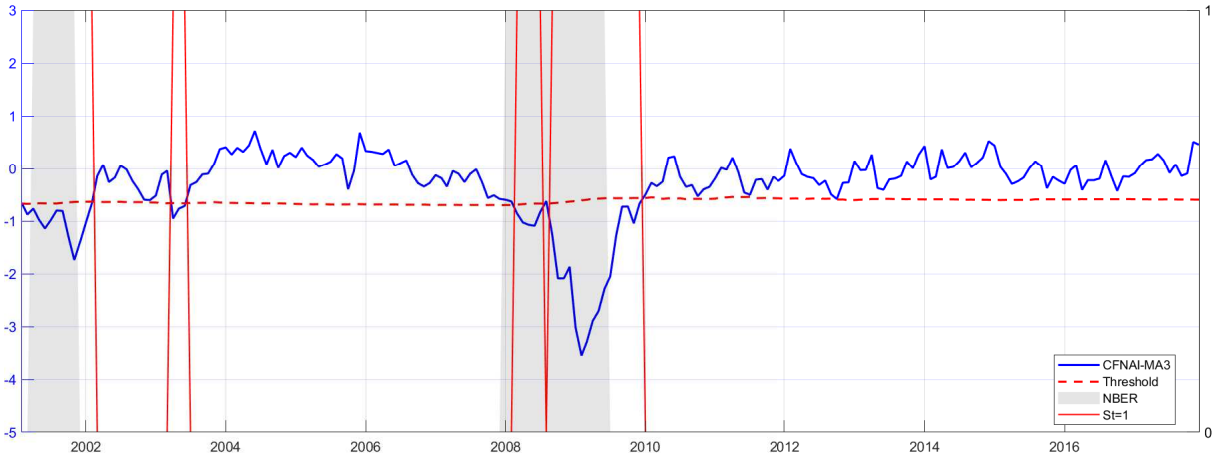

Notes: Panel (a) corresponds to the in-sample estimation of the final data vintage 1967M4-2017M12. Panel(b) corresponds to the real-time recursive out-of-sample nowcasts 2001M2-2017M12. Hence, each point t on the x-axis corresponds to the information set as of period t. The solid and the dashed red line denote the mode and mean of the posterior densities of the recession regime $S_t = 1$ and the threshold value r, respectively. The blue solid line displays the three-month-moving average of the Chicago Fed National Activity Index. Shaded areas correspond to the recessions dated by the NBER.

4.2 In-sample Results

Table 2 displays the posterior mean of the shrinkage parameters. According to equation (15), a lower value for λ_i is associated with stronger shrinkage. Four points deserve to be stressed here. First, the amount of shrinkage increases with model size as in Bańbura et al. (2010). Second, there is strong cross-variable shrinkage which is in line with Carriero et al. (2015a). Third, the shrinkage for the business cycle variables, CFNAI and CSVM, is less than for the remaining variables. This is a first indication of the importance of those variables for accurate forecasts. And fourth, there is a stronger overall shrinkage and less cross-variable shrinkage in the recession regime implying that information emerging from other variables can be crucial for forecasts during recessions where information coming from their own past is more important in expansions.

Table 2: Shrinkage

		MF	MF-CSVM	MF-T	MF-T-CSVM	MF^{med}	MF-$CSVM^{med}$	MF^{b}
		Overall, Cross-Variable and BC Shrinkage						
λ_1	$S_t = 1$	0.275	0.181	0.131	0.069	0.112	0.120	0.096
	$S_t = 2$			0.208	0.162			
$\lambda_1\lambda_2$	$S_t = 1$	0.005	0.002	0.007	0.003	0.003	0.002	0.010
	$S_t = 2$			0.003	0.002			
$\lambda_1\lambda_3$	$S_t = 1$	0.028	0.016	0.038	0.016	-	0.042	-
	$S_t = 2$			0.035	0.015			

Notes: λ_i refers to posterior mean and $\lambda_i\lambda_j$ to posterior mean of the product. A larger value implies less shrinkage. Since the medium-scale MF^{med} and benchmark MF^{b} do neither contain the CFNAI index nor the CSVM, they do not include any BC shrinkage via λ_3. $S_t = 1$ identifies the recession regime.

Figure 2 shows the common stochastic volatility for the final vintage for the MF-CSVM-VAR and the MF-T-CSVM-VAR. Both models show qualitatively similar results. Though, the values for the MF-T-CSVM-VAR are somewhat smaller during recessions since the model accounts for the difference in scaling across business cycle regimes due to $\Sigma_1 \neq \Sigma_2$ in equation (13). Up to 1987 one can observe a period of high volatility with its peak around the recession 1980-1981. The prolonged period of low volatility from 1987 until 2007 is referred to as the Great Moderation. The Great Recession induce another strong increase in volatility around 2008/2009 followed by a subsequent slow-down to levels similar to the Great Moderation. This supports the finding of Clark (2009) that the Great Recession only interrupts the Great Moderation, but does not end it. Overall, the pattern closely follows the macroeconomic uncertainty index by Jurado et al. (2015). Hence, the volatility factor corresponds closely to the macroeconomic uncertainty which spikes upwards in most recessions. This pattern is also well reflected in the volatility of the monthly GDP estimates (see Figure 6 in Appendix D).

Figure 2: Common Stochastic Volatility

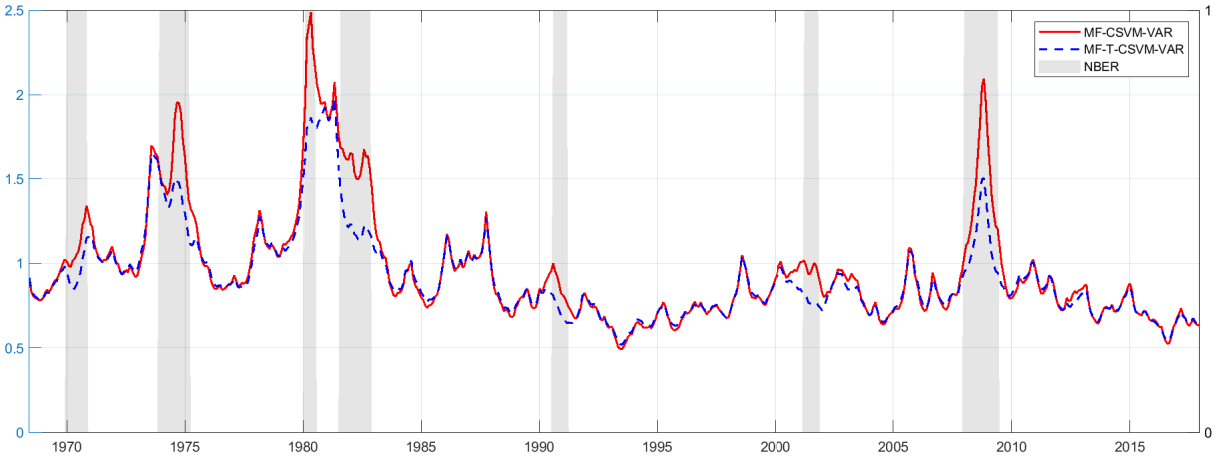

Notes: The lines indicate the posterior mean from the common stochastic volatility factor f_t as standard deviations. The red solid line and blue dashed line refer to MF-CSVM-VAR and MF-T-CSVM-VAR, respectively, from the final data vintage. Shaded areas correspond to the recessions dated by the NBER. Sample: 1967M4-2017M12.

4.3 Point Forecast Evaluation

The point forecast accuracy is measured as the root-mean-squared error (RMSE):

$$\text{RMSE}_h^M = \sqrt{\frac{1}{T_f}\sum_t \left(y_{t+h} - \hat{y}_{t+h}^M\right)^2} \tag{17}$$

relative to the benchmark model:

$$\text{relative RMSE}_h^M = \frac{\text{RMSE}_h^M}{\text{RMSE}_h^b}, \tag{18}$$

where M denotes the model, b the benchmark model, $\hat{y}_{t+h}$ the posterior mean as the point forecast, y_{t+h} the actual value and T_f the recursive sample size. I apply a Diebold-Mariano test with Newey-West standard errors to roughly gauge the statistical significance of the results. GDP is measured in annualized percentage changes for comparison with the SPF in Section 4.5.

Table 3 displays the relative RMSE for the full out-of-sample period. The best performance on average across all horizons and variables is obtained for the MF-T-CSVM-VAR with a reduction of 11% in relative RMSEs. The MF-T-VAR shows the highest relative forecasting accuracy in terms of nowcasting. In contrast, both medium-scale VARs reveal their strength with increasing forecasting horizon. The CSVM contributes the most for forecast horizons exceeding the nowcast $h > 1$ and for the UR.

For GDP, we can observe a significant gain in nowcast accuracy with regard to the MF-VAR and MF-T-VAR by 12%. The MF-CSVM-VAR^{med} reveals the best accuracy with gains up to 15% for horizons $h > 1$. In terms of CPI, only models that include CSVM can significantly improve the benchmark, whereas the relative improvements are rather moderate with maximum 9%. In contrast, the relative improvements for UR are the largest, though they are rarely significant.

Of notable mention here is the MF-T-CSVM-VAR with relative gains up to 22%. Again, the MF-T-VAR shows a strong performance for the nowcast.

Table 3: Relative RMSEs

Model	h=1	h=2	h=3	h=4
	GDP			
MF-VAR	**0.88*****	0.91***	0.93***	0.98**
MF-CSVM-VAR	0.93	0.90**	0.90***	0.95**
MF-T-VAR	0.88***	0.92**	0.91***	0.93***
MF-T-CSVM-VAR	0.90***	0.90**	0.88***	0.92***
MF-VAR^{med}	0.90*	0.88**	0.86*	0.87**
MF-CSVM-VAR^{med}	0.93	**0.87*****	**0.85*****	**0.86*****
MF-VAR^{b}	*0.50*	*0.63*	*0.68*	*0.67*
	Inflation			
MF-VAR	1.00	1.03	0.99	0.99
MF-CSVM-VAR	0.99	0.97***	0.95***	0.96***
MF-T-VAR	**0.97**	1.01	1.00	0.99
MF-T-CSVM-VAR	0.98	**0.96***	0.97	0.96**
MF-VAR^{med}	0.99	0.98	0.96	0.94
MF-CSVM-VAR^{med}	0.98**	0.97*	**0.94****	**0.91*****
MF-VAR^{b}	*0.21*	*0.29*	*0.28*	*0.28*
	Unemployment Rate			
MF-VAR	0.92	0.88	0.89	0.90*
MF-CSVM-VAR	0.89	0.80*	**0.79***	**0.80****
MF-T-VAR	**0.84***	0.84*	0.88*	0.90*
MF-T-CSVM-VAR	0.85	**0.78***	0.80*	0.81*
MF-VAR^{med}	1.00	1.03	1.07	1.09
MF-CSVM-VAR^{med}	1.00	0.97	0.96	0.96
MF-VAR^{b}	*0.16*	*0.39*	*0.63*	*0.87*

Notes: The relative RMSEs are expressed as ratios relative to the benchmark model. A figure below unity indicates that the model outperforms the benchmark. The benchmark is reported in absolute terms in italic figures (the last column of each panel). Bold figures indicate the best performance for the variable and horizon. *, **and ***denote significance at the 10%, 5% and 1% level, respectively, according to the Diebold-Mariano test with Newey-West standard errors. GDP is measured in annualized growth rates. Out-of-sample: 2001M2-2017M12.

Since the paper emphasizes the relationship between the state of the business cycle and forecasting, it is of particular interest to examine the two regimes, recession and expansion, separately. Therefore, I divide the sample into two subsamples consistent with the recession and expansion dates according to the NBER business cycle dating committee. The left and right panel of Table 4 present the relative RMSE for the recession and expansion subsample, respectively. For the recessions, the highest precision across all horizons and variables on average is shown by the MF-T-CSVM-VAR with a reduction of 15% in relative RMSEs which improved by 4% compared to the full sample. Moreover, two additional results stand out. First, the relative nowcast precision of the T-VARs increased even more for GDP and UR compared to the full sample. The MF-T-VAR is best for GDP with a reduction of 15%. The MF-T-CSVM-VAR reduces the relative RMSE of UR by 38%. Second, gains in forecast accuracy for the CPI are

again rather moderate and often insignificant. However, it is a different story for the expansion subsample. The MF-CSVM-VAR works well with a drop of 4% in relative RMSE on average over all variables and horizons. It is also noticeable that every model with CSVM beats its counterpart without CSVM during expansions with largest gains again for the UR.

Table 4: Relative RMSEs for Recessions and Expansions

	NBER Recessions				NBER Expansions			
Model	h=1	h=2	h=3	h=4	h=1	h=2	h=3	h=4
	GDP							
MF-VAR	0.93**	0.92	0.93**	0.97**	**0.86*****	0.90***	0.93***	0.99
MF-CSVM-VAR	1.05	0.92	0.90**	0.93***	0.88***	0.89**	0.91**	0.97
MF-T-VAR	**0.85*****	0.94**	0.93	0.91**	0.90**	0.90*	0.89***	0.94
MF-T-CSVM-VAR	0.91**	**0.91**	**0.88****	0.90**	0.90**	0.89*	0.88***	0.93*
MF-VAR^{med}	0.93	0.92	0.90	0.87	0.89	0.84**	0.83*	0.86
MF-CSVM-VAR^{med}	0.98	0.94	0.89	**0.87****	0.92	**0.82*****	**0.82****	**0.85****
MF-VAR^{b}	*0.75*	*1.13*	*1.29*	*1.27*	*0.45*	*0.51*	*0.53*	*0.53*
	Inflation							
MF-VAR	1.03	1.06	1.03	1.01	0.98***	0.99	0.96***	0.97***
MF-CSVM-VAR	1.02	0.99	**0.97*****	0.98*	0.96***	0.93***	0.94***	0.94***
MF-T-VAR	**0.96**	1.04	1.04	1.01	0.99	0.97	0.96**	0.96**
MF-T-CSVM-VAR	0.98	**0.99**	0.98	0.98	0.98	0.93**	0.95**	0.95**
MF-VAR^{med}	1.01	1.03	1.02	0.98	0.96***	**0.92*****	0.90***	0.90**
MF-CSVM-VAR^{med}	1.01	1.00	0.98	**0.95**	**0.96*****	0.92***	**0.90*****	**0.88*****
MF-VAR^{b}	*0.41*	*0.60*	*0.54*	*0.52*	*0.16*	*0.20*	*0.22*	*0.22*
	Unemployment Rate							
MF-VAR	0.72**	0.75**	0.80***	0.83***	1.04	1.05	1.08	1.05
MF-CSVM-VAR	0.66**	0.64**	0.69***	0.73***	1.02	0.99	**0.99**	**0.95**
MF-T-VAR	0.64*	0.73**	0.80***	0.83***	**0.96**	**0.97**	1.05	1.06
MF-T-CSVM-VAR	**0.61***	**0.61****	**0.68*****	**0.72*****	0.98	0.99	1.04	1.02
MF-VAR^{med}	0.82*	0.80*	0.78**	0.77**	1.11*	1.30***	1.57***	1.67***
MF-CSVM-VAR^{med}	0.94	0.87	0.84*	0.83**	1.04	1.09	1.22**	1.26***
MF-VAR^{b}	*0.29*	*0.84*	*1.48*	*2.07*	*0.13*	*0.26*	*0.36*	*0.48*

Notes: The relative RMSEs are expressed as ratios relative to the benchmark model. A figure below unity indicates that the model outperforms the benchmark. The benchmark is reported in absolute terms in italic figures (the last column of each panel). Bold figures indicate the best performance for the variable and horizon. *, **and ***denote significance at the 10%, 5% and 1% level, respectively, according to the Diebold-Mariano test with Newey-West standard errors. GDP is measured in annualized growth rates. The left and right panel refers to periods that the NBER identifies as recessions and expansions, respectively. Out-of-sample: 2001M2-2017M12.

Since the results with respect to the business cycle regimes indicate a significant difference in forecast performance for GDP and UR, it is of peculiar interest to examine the development of the relative RMSE over time for both variables. Thereby, I focus on the nowcast of GDP and UR as they reveal the largest gains in recessions. Figure 3 depicts the cumulative sum of RMSE for the nowcast of GDP and UR. I subtract the cumulative sum of the benchmark model such that positive values indicate a better performance and the benchmark is indicated by a zero line.

Regarding GDP, the MF-T-VAR improves upon all models during and following the first

recession in 2001. Thereafter, the accuracy converges among all models up to the point that they fail to beat the benchmark. All models start to improve after 2006 but diverge considerably with the start of the Great Recession, more specifically, during the largest decline of GDP in 2008Q4 in which the MF-T-VAR outperforms all other models by quite a margin. One can see another large kink in the first quarter of 2011 during which the GDP slumps by roughly 1%. Though, in this occasion all models equally enhance relative the benchmark.

In contrast, UR depicts a more stable pattern. Right from the first sharp increase in the UR in the middle of 2001, the MF-T-VAR starts to steadily improve upon all other models, with a sharp increase again during the Great Recession. Following the Great Recession, all linear models decline relative to the benchmark, whereas both T-VARs maintain their relative levels. This decline in forecast accuracy is particularly striking for both medium-scale VARs during the long recovery in the labour market following the Great Recession.

In summary, the MF-T-VAR and MF-T-CSVM-VAR provide by far the most accurate nowcasts during recessions, with the nowcast for GDP and UR clearly standing out. This gains are mainly driven by deteriorating times during the recession periods, in particular the severe conditions during the Great Recession. This shows that it is important to timely incorporate information on the current state of the business cycle into forecasting models for point forecasts of GDP and UR–however CPI does not benefit from it. Accounting for time-varying macroeconomic uncertainty in form of CSVM increases point forecast accuracy for forecast horizons beyond the nowcast on average over all variables–notably for UR during recessions. The medium-scale MF-CSVM-VAR^{med} reveals precise forecasts for GDP and CPI for horizons exceeding the nowcast $h > 1$.

4.4 Density Forecast Evaluation

Recently more and more interest and importance in the literature on forecasting is shifted towards density forecasts to account for the uncertainty surrounding point forecasts (see Wright, 2019). I employ the continuous ranked probability score (CRPS) introduced by Matheson and Winkler (1976) to evaluate the entire forecast density. I follow Gneiting and Ranjan (2011) and apply the score function:

$$S(p_t^M, y_{t+h}, \nu(u)) = \int_{-0}^{1} \mathrm{QS}_u(P_t^M(u)^{-1}, y_{t+h})\nu(u)du, \tag{19}$$

where $\mathrm{QS}_u(P_t^M(u)^{-1}, y_{t+h}) = 2(I\{y_{t+h} < P_t^M(u)^{-1}\} - u)(P_t^M(u)^{-1} - y_{t+h}^M)$ is the quantile score for forecast quantile $P_t^M(u)^{-1}$ of model M at level $0 < u < 1$. $I\{y_{t+h} < P_t^M(u)^{-1}\}$ denotes an indicator function which is one in case of $y_{t+h} < P_t^M(u)^{-1}$ and zero otherwise. p_t^M denotes the predictive density and $(P_t^M)^{-1}$ the inverse of the cumulative predictive density for model M. $\nu(u)$ is a weighting function. I use a simple uniform weighting scheme $\nu(u) = 1$. Thus, the average CRPS is:

$$\mathrm{CRPS}_h^M = \frac{1}{T_f} \sum_t S(p_t^M, y_{t+h}, 1). \tag{20}$$

Figure 3: Relative Cumulative Sum of Squared Nowcast Errors

(a) GDP

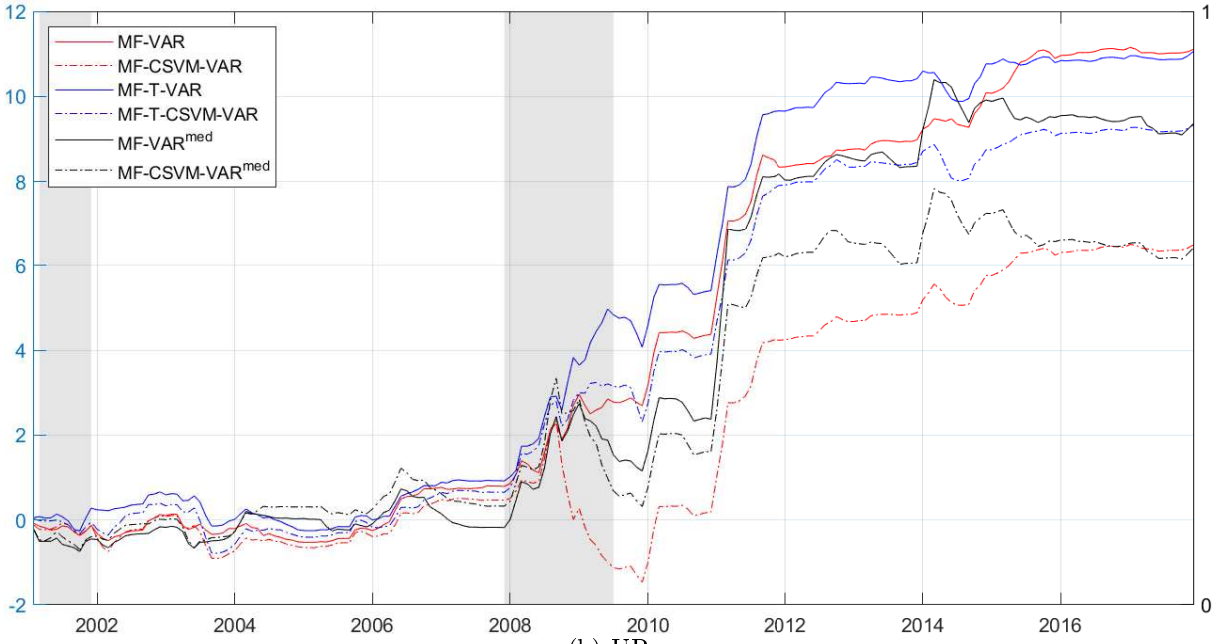

(b) UR

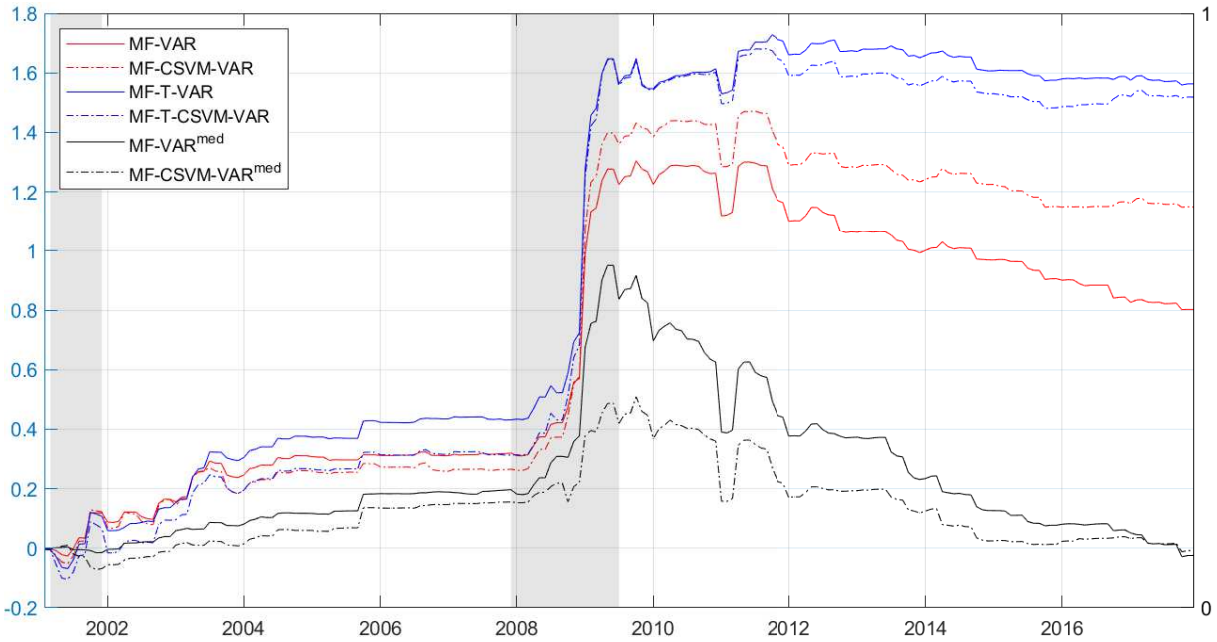

Notes: Lines refer to the relative cumulative sum of squared forecast errors at horizon $h = 1$ in difference to the benchmark. A value above zero indicates a better forecast accuracy. GDP is measured in annualized growth rates. Shaded areas correspond to the recessions dated by the NBER. Out-of-sample: 2001M2-2017M12

A lower value signifies a better fit of the predictive density with respect to the true data density. I evaluated the CRPS as a ratio relative to the benchmark:

$$\text{relative CRPS}_h^M = \frac{CRPS_h^M}{CRPS_H^b} \tag{21}$$

To gauge equal predictive forecast accuracy, I regress the differences between the CRPS and the benchmark on a constant. Inference is based on a t-test with Newey-West standard errors.

Table 5 shows the relative CRPS for the entire sample and Table 6 displays the results conditional on the business cycle state according the NBER chronology. The overall result of the density forecasts support the results of the point forecasts in Section 4.3. On average over all variables and horizons, the MF-T-CSVM-VAR still beats all other models with a decline of 11% in CRPS. The result enhances to an overall reduction of 18% during recessions. While the MF-T-CSVM-VAR still performs best during expansions, the reduction in relative CRPS is lower with 8%.

Similar to the point forecasts, the best performance for the nonlinear MF-T-VAR and MF-T-CSVM-VAR is during the recession periods for the nowcast of GDP and UR. However, the difference for the MF-T-VAR to the benchmark for GDP is even larger with a decline in the relative CRPS by 19% compared to 15%. The same holds for the MF-T-CSVM-VAR for UR, though the incline from 39% to 41% is only minor. Furthermore, the improvement due to CSVM in recessions for forecast horizons $h > 1$ is even more pronounced for each model. Thus, the contribution of adding CSVM is best when analysing the whole predictive density as it takes into account the change in volatility over time.

All in all, the results from the density forecast evaluation confirmed the point forecast results. For GDP and UR, one can achieve even better results in terms of the nowcasts during recessions. Therefore, the MF-T-VAR and MF-T-CSVM-VAR can also very well reflect the uncertainty surrounding the point forecast that is associated with periods of high volatility during recessions. The CSVM feature again works particularly well for forecast horizons exceeding the nowcast $h > 1$ but is even more pronounced.

4.5 Nowcast Comparison with the Survey of Professional Forecasters

In general, any forecasting model has a hard time to beat survey or institutional forecasts (see discussion in Wright, 2019). Nevertheless, these forecasts also perform rather poorly for GDP during recessions (see, i.e., Dovern and Jannsen, 2017; Sinclair, 2019). With promising results for the GDP nowcast from the MF-T-VAR during recessions, it is worth comparing this model's nowcast against the Survey of Professional Forecasters (SPF) from the Federal Reserve Bank of Philadelphia.

The SPF has two limitations for an exact evaluation against the MF-T-VAR. First, the SPF reports only once a quarter and hence, I can compare it only on a quarterly basis which cuts the out-of-sample period to 64 observations. Second, it is difficult to exactly match the information set with the corresponding SPF deadlines in real-time. The questionnaires are send to the participants at the end of the first month of each quarter at the time of the publication of the Bureau of Economic Analysis' advance report. The deadline to submit the forecasts is at late in the second to third week of the second month of each quarter. Hence, the information set for the SPF is in between the end of the first and end of the second month, though the exact timing depends on the date of submission of each participant. As the CFNAI is crucial for the MF-T-VAR and is only published at the end of each month, I compare it against the SPF

Table 5: Relative CRPS

Model	h=1	h=2	h=3	h=4
	GDP			
MF-VAR	0.89***	0.90***	0.94***	0.98***
MF-CSVM-VAR	0.91***	0.88***	0.89***	0.94***
MF-T-VAR	**0.88****	0.89***	0.92***	0.94***
MF-T-CSVM-VAR	0.89***	0.87***	0.87***	0.91***
MF-VAR^{med}	0.93**	0.88**	0.88*	0.89**
MF-CSVM-VAR^{med}	0.94*	**0.86****	**0.85****	**0.86****
MF-VAR^{b}	*0.27*	*0.33*	*0.36*	*0.35*
	Inflation			
MF-VAR	1.00	1.03	0.99	0.99
MF-CSVM-VAR	0.98*	**0.94****	0.92***	0.92***
MF-T-VAR	0.98	1.00	0.98	0.98
MF-T-CSVM-VAR	0.98	0.95*	0.93***	0.93***
MF-VAR^{med}	0.98**	0.97	0.95	0.93
MF-CSVM-VAR^{med}	**0.97****	0.95***	**0.91****	**0.88****
MF-VAR^{b}	*0.11*	*0.14*	*0.14*	*0.14*
	Unemployment Rate			
MF-VAR	0.97	0.93	0.92*	0.92
MF-CSVM-VAR	0.92*	0.84***	0.80***	**0.79****
MF-T-VAR	**0.88****	0.85***	0.87***	0.87***
MF-T-CSVM-VAR	0.88***	**0.82****	**0.80****	0.80***
MF-VAR^{med}	1.02	1.11*	1.22**	1.29***
MF-CSVM-VAR^{med}	0.99	0.99	1.03	1.05
MF-VAR^{b}	*0.09*	*0.20*	*0.31*	*0.43*

Notes: The relative CRPS are expressed as ratios relative to the benchmark model. A figure below unity indicates that the model outperforms the benchmark. The benchmark is reported in absolute terms in italic figures (the last column of each panel). Bold figures indicate the best performance for the variable and horizon. *, **and ***denote significance at the 10%, 5% and 1% level, respectively, according to the difference in mean test with Newey-West standard errors. GDP is measured in annualized growth rates. The out-of-sample goes from 2001M2-2017M12.

across the three information sets–I1, I2 and I3 defined as the end of the first, second and third month of each quarter, respectively. Hence, the MF-T-VAR starts each quarter with I1 with an information disadvantage of roughly two to three weeks against the SPF. This information set does not contain a value for the CFNAI concerning the current quarter as it has a publication lag of one month. The information set continues with I2 with an advantage of an additional week of data releases which includes the first figure of the CFNAI of the current quarter. The final set I3 takes the whole current quarter into account.

Table 7 shows the nowcast errors relative to the SPF. For the full sample, there is an increase in accuracy with incoming information. For I1, with an information disadvantage, the MF-T-VAR performs worse than the SPF but breaks even with new information in I2 and I3. For recessions, the MF-T-VAR beats the SPF already in I1 with gains increasing from 9% up to 29% with incoming new information at the end of the each month. On the contrary, the SPF dominates the expansion subsample independent of the information set.

Table 6: Relative CRPS for Recessions

Model	NBER Recessions h=1	h=2	h=3	h=4	NBER Expansions h=1	h=2	h=3	h=4
	GDP							
MF-VAR	0.95	0.93	0.92***	0.96**	**0.87*****	0.89***	0.94***	0.99**
MF-CSVM-VAR	1.00	0.90	0.91	0.94	0.88***	0.87***	0.88***	0.94**
MF-T-VAR	**0.81*****	0.94**	0.94	0.91**	0.90***	0.88***	0.91***	0.95**
MF-T-CSVM-VAR	0.87***	**0.89**	**0.89****	0.91**	0.90***	0.86***	0.87***	0.91***
MF-VAR^{med}	0.92	0.95	0.92	**0.86**	0.93*	0.86***	0.87*	0.89
MF-CSVM-VAR^{med}	0.93	0.95	0.92	0.86*	0.95	**0.83*****	**0.83*****	**0.86*****
MF-VAR^{b}	*0.46*	*0.64*	*0.75*	*0.72*	*0.25*	*0.29*	*0.30*	*0.30*
	Inflation							
MF-VAR	1.05	1.11*	1.08	1.06	0.98***	0.99	0.96***	0.97***
MF-CSVM-VAR	0.97	**0.96**	**0.96**	1.01	0.98	0.94***	0.90***	0.89***
MF-T-VAR	**0.94**	1.05	1.08*	1.07**	0.99	0.97	0.95***	0.96***
MF-T-CSVM-VAR	0.94	0.98	0.98	1.02	0.99	0.94***	0.91***	0.90***
MF-VAR^{med}	1.02	1.09**	1.10	1.06	**0.96*****	0.92***	0.91***	0.90**
MF-CSVM-VAR^{med}	0.98	1.01	1.00	**0.99**	0.97**	**0.92*****	**0.88*****	**0.85*****
MF-VAR^{b}	*0.21*	*0.32*	*0.27*	*0.23*	*0.09*	*0.11*	*0.12*	*0.13*
	Unemployment Rate							
MF-VAR	0.75***	0.72***	0.74***	0.77***	1.04	1.03	1.04	1.03
MF-CSVM-VAR	0.63***	0.58***	0.61***	0.65***	1.02	0.97	**0.94**	**0.89****
MF-T-VAR	0.63***	0.67***	0.73***	0.76***	**0.96**	**0.95**	0.96	0.96
MF-T-CSVM-VAR	**0.59*****	**0.55*****	**0.59*****	**0.64*****	0.98	0.96	0.94	0.92
MF-VAR^{med}	0.82***	0.80**	0.77**	0.76**	1.09*	1.26***	1.53***	1.68***
MF-CSVM-VAR^{med}	0.88**	0.85*	0.82*	0.80*	1.03	1.06	1.17**	1.24***
MF-VAR^{b}	*0.17*	*0.53*	*1.00*	*1.45*	*0.07*	*0.15*	*0.21*	*0.29*

Notes: The relative CRPS are expressed as ratios relative to the benchmark model. A figure below unity indicates that the model outperforms the benchmark. The benchmark is reported in absolute terms in italic figures (the last column of each panel). Bold figures indicate the best performance for the variable and horizon. *, **and ***denote significance at the 10%, 5% and 1% level, respectively, according to the difference in mean test with Newey-West standard errors. GDP is measured in annualized growth rates. The left and right panel refers to periods that the NBER identifies as recessions and expansions, respectively. Out-of-sample: 2001M2-2017M12.

Table 7: RMSEs for GDP Nowcast relative to SPF

	I1	I2	I3	I1	I2	I3	I1	I2	I3
	Full sample			Recessions			Expansions		
MF-T-VAR	1.06	1.00	0.98	0.91	0.85	0.71	1.15	1.10	1.12

Notes: The relative RMSEs are expressed as ratios relative to the SPF. A figure below unity indicates that the model outperforms the benchmark. Out-of-sample: 2001M2-2017M12.

Figure 4 displays the GDP nowcast errors (bars) for the SPF and the MF-T-VAR for I1, I2 and I3 together with the annualized GDP growth rates (solid line). The sequence of bars at each point in time is ordered as SPF, I1, I2 and I3. Errors are defined as actual minus forecast $y_{(t+h)} - \hat{y}_{(t+h)}$. Hence, negative errors indicate a too optimistic forecast for negative growth rates

and too pessimistic forecast for positive growth rates. Thus, if the MF-T-VAR beats the SPF and new information reduces nowcast errors, the bars should ascend (descend) for negative (positive) errors from left to right at a specific point in time. Overall, the SPF and MF-T-VAR tend to make the similar nowcast errors over time with a correlation of 0.85, 0.87 and 0.85 for I1, I2 and I3, respectively. 2001Q3, 2008Q1 and 2008Q4 render the steepest downturns with negative forecast errors in the full sample coinciding with recessions. Thus, both the MF-T-VAR as well as the SPF are too optimistic in downturns during recessions. However, in both occasions the negative forecast error is lower for the MF-T-VAR. This is already present for I1 and decreased even further with more information in I2 and I3–particularly evident for the largest forecast error in 2008Q4. On the contrary, large negative forecast errors present in expansion, i.e. first quarter of 2011 with annualized GDP growth of -1.5%, can not be diminished by the M-T-VAR.

Overall, the MF-T-VAR can help to lower systematic negative nowcast errors made by SPF in recessions as described by Dovern and Jannsen (2017), though in expansions the SPF is still a benchmark hard to beat. For information on other models and forecast horizons I refer to Figure 7 in Appendix D. In short, the medium-scale MF-VARs can keep up with the SPF concerning GDP for forecast horizons $h > 1$ and even perform better by small margin for $h = 4$.

Figure 4: Nowcast Errors - SPF against MF-T-VAR

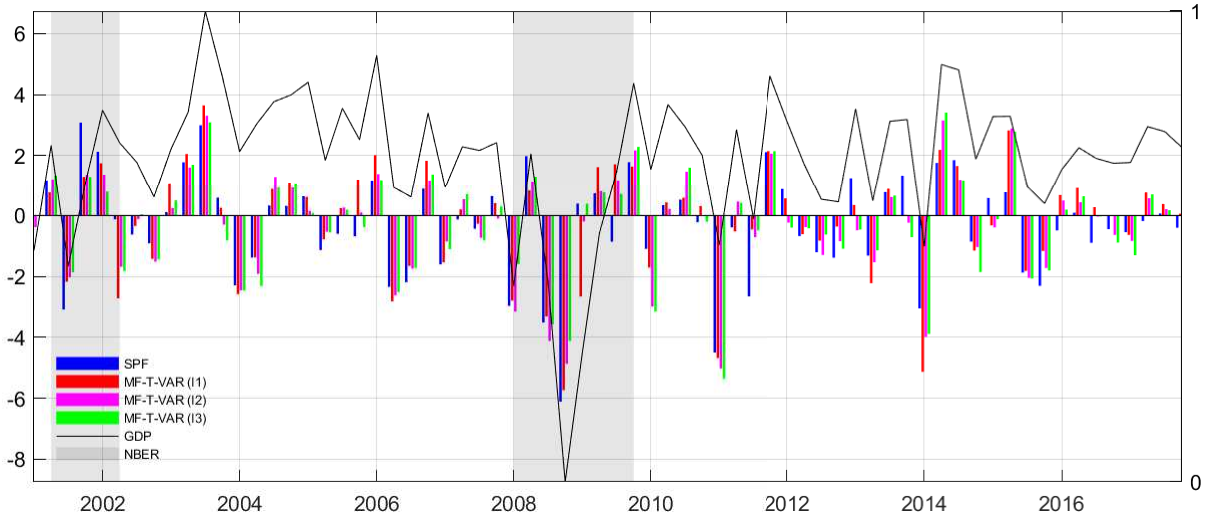

Notes: The black solid line refers to actual GPD in annualized growth rates. The forecast errors are defined as $(y_{t+h} - \hat{y}_{t+h})$ for $h = 1$. Hence, a negative value indicates that the forecast is too optimistic for negative GDP growth rates. The blue, red, magenta and green bars refer to the nowcast error of the SPF and MF-T-VAR for information set I1, I2 and I3, respectively. Shaded areas correspond to the recessions dated by the NBER. Out of sample: 2001Q1 - 2017Q4

4.6 Nowcasting during the Great Recession

Unsurprisingly, the largest forecast errors according to Figure 4 occur in 2008Q4 during the Great Recession with the largest drop in GDP. Thus, it is of great interest how the different models and the SPF perform during that time in detail. Figure 5 presents the entire nowcast densities together with point nowcasts and the actual GDP value. Each panel includes the different

monthly information sets. Hence, I1, I2 and I3 refer to 2008M10, 2008M11 and 2008M12.

There are two main results to consider. First, all models with CSVM show significant wider tails in the predictive density. Thus, the time-varying volatility clearly takes the heightened uncertainty during that time into account and thus, enhances density nowcasts. Second, for MF-T-VAR, MF-T-CSVM-VAR and MF-VAR, all dashed-dotted lines are left of the dashed line and right of the solid line, denoting means of the forecast densities, SPF nowcast and final GDP value, respectively. Hence, these models nowcast better than the SPF from information set I1 onward. Overall, if a forecaster is interested in both point and density forecasts, it is best to include information about the business cycle in form of an index, regime dependent parameters and additionally account for macroeconomic uncertainty in form of common time-varying volatility.

Figure 5: GDP Nowcast Densities for 2008Q4 during the Great Recession

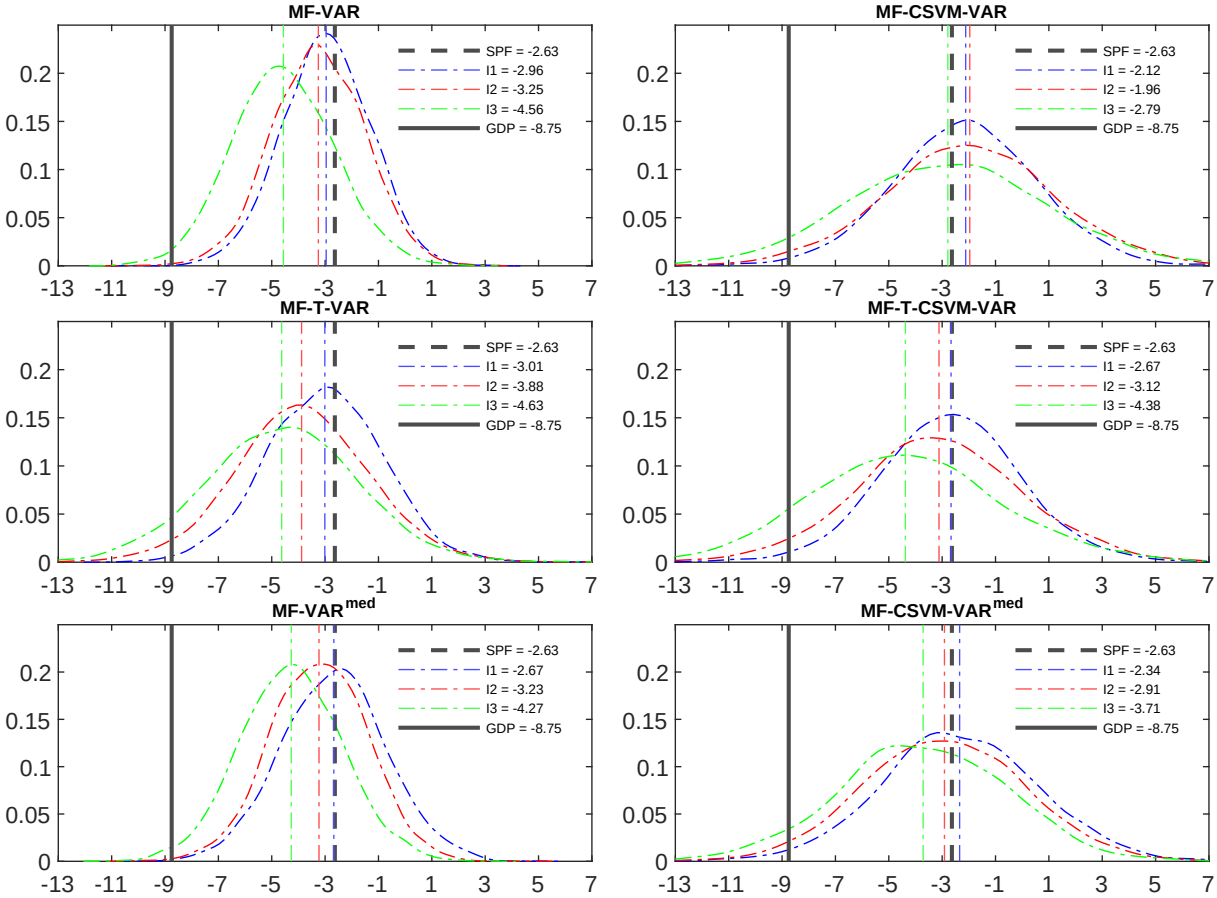

Notes: Figures refer to each model with its nowcast densities (based on a normal kernel density estimate) and the respective mean (dashed-dotted line). Within each figure, the blue, the red and the green dashed-dotted line refer to 2008M10, 2008M11 and 2008M12 vintage, respectively. The SPF nowcast is shown by a black dashed line while the final value for GDP by a black solid line.

5 Conclusion

Macroeconomists have a hard time to forecast and even nowcast during recessions. Especially following the Great Recession in 2008/09, this problem has aroused interest in recent research on

forecasting. To approach this problem, this paper proposes a novel VAR that can handle mixed-frequency data and recurring business cycle regimes and common stochastic volatility in mean as important business cycle features in real-time. To this end, I combined a mixed-frequency VAR (MF-VAR) with a threshold VAR (T-VAR) which additionally accounts for time-varying macroeconomic uncertainty in form of common stochastic volatility in mean (CSVM). I utilize the Chicago Fed National Activity Index as business cycle index for the threshold variable to date the business cycle in real-time. A Minnesota prior is used for all VARs where the shrinkage parameter is estimated with an adaptive Normal-inverse-Gamma prior. This allows to determine the amount of shrinkage and furthermore permits for different shrinkage across business cycle regimes and variables.

In a real-time forecasting experiment for US GDP, CPI and UR, the MF-T-CSVM-VAR outperforms on average across all variables and horizons linear MF-VARs without the business cycle features of different size with respect to point and density forecasts. The difference in performance is especially pronounced for nowcasts for GDP and UR during recessions. The MF-T-VAR even reduces GDP nowcast errors made by the Survey of Professional Forecasters (SPF) during the sharp drop in economic activity of 2008Q4 during the Great Recession. Thus, the results suggest that it is valuable for the short-term forecast during recessions to identify the current state of the economy and incorporate this information into the model. By contrast, the medium-scale MF-CSVM-VAR reveals accurate GDP forecasts for horizons of two to four quarters ahead in which case it is quite competitive to the SPF. The time-varying volatility CSVM provides the largest gains for UR forecasts–notably density forecasts for two to four quarters ahead.

References

Aastveit, K. A., A. Carriero, T. E. Clark, and M. Marcellino (2017). Have standard VARs remained stable since the crisis? Journal of Applied Econometrics 32(5), 931–951.

Alessandri, P. and H. Mumtaz (2017). Financial conditions and density forecasts for US output and inflation. Review of Economic Dynamics 24, 66–78.

Auerbach, A. J. and Y. Gorodnichenko (2012). Measuring the Output Responses to Fiscal Policy. American Economic Journal: Economic Policy 4(2), 1–27.

Bańbura, M., D. Giannone, and L. Reichlin (2010). Large Bayesian vector auto regressions. Journal of Applied Econometrics 25(1), 71–92.

Barnett, A., H. Mumtaz, and K. Theodoridis (2014). Forecasting UK GDP growth and inflation under structural change. A comparison of models with time-varying parameters. International Journal of Forecasting 30(1), 129–143.

Barsoum, F. and S. Stankiewicz (2015). Forecasting GDP growth using mixed-frequency models with switching regimes. International Journal of Forecasting 31(1), 33–50.

Berge, T. J. and O. Jorda (2011). Evaluating the Classification of Economic Activity into Recessions and Expansions. American Economic Journal: Macroeconomics 3(2), 246–77.

Bessec, M. and O. Bouabdallah (2015). Forecasting GDP over the business cycle in a multi-frequency and data-rich environment. Oxford Bulletin of Economics and Statistics 77(3), 360–384.

Bloom, N. (2014). Fluctuations in uncertainty. The Journal of Economic Perspectives 28(2), 153–175.

Brave, S. (2009). The Chicago Fed National Activity Index and business cycles. Chicago Fed Letter (268), 1.

Brave, S. and R. A. Butters (2010). Chicago Fed National Activity Index turns ten-analyzing its first decade of performance. Chicago Fed Letter (273), 1.

Brave, S. A. and R. Butters (2014). Nowcasting using the Chicago Fed National Activity Index. Economic Perspectives 38(1).

Caggiano, G., E. Castelnuovo, and N. Groshenny (2014). Uncertainty shocks and unemployment dynamics in US recessions. Journal of Monetary Economics 67(C), 78–92.

Carriero, A., T. E. Clark, and M. Marcellino (2015a). Bayesian VARs: specification choices and forecast accuracy. Journal of Applied Econometrics 30(1), 46–73.

Carriero, A., T. E. Clark, and M. Marcellino (2015b). Realtime nowcasting with a Bayesian mixed frequency model with stochastic volatility. Journal of the Royal Statistical Society: Series A 178(4), 837–862.

Carriero, A., T. E. Clark, and M. Marcellino (2016). Common Drifting Volatility in Large Bayesian VARs. Journal of Business & Economic Statistics 34(3), 375–390.

Carriero, A., T. E. Clark, and M. Marcellino (2018). Measuring uncertainty and its impact on the economy. Review of Economics and Statistics 100(5), 799–815.

Carriero, A., A. B. Galvao, and G. Kapetanios (2019). A comprehensive evaluation of macroeconomic forecasting methods. International Journal of Forecasting 35(4), 1226–1239.

Carstensen, K., M. Heinrich, M. Reif, and M. H. Wolters (2020). Predicting ordinary and severe recessions with a three-state markov switching dynamic factor model. An application to the German business cycle. International Journal of Forecasting Forthcoming.

Carter, C. K. and R. Kohn (1994). On Gibbs Sampling for State Space Models. Biometrika 81(3), 541–553.

Chauvet, M. and S. Potter (2005). Forecasting recessions using the yield curve. Journal of Forecasting 24(2), 77–103.

Chauvet, M. and S. Potter (2013). Forecasting output. Handbook of Economic Forecasting 2(Part 1), 141–194.

Chen, C. W. and J. C. Lee (1995). Bayesian inference of threshold autoregressive models. Journal of Time Series Analysis 16(5), 483–492.

Clark, T. E. (2009). Is the Great Moderation over? An empirical analysis. Economic Review (Q IV), 5–42.

Clark, T. E. (2011). Real-time density forecasts from Bayesian vector autoregressions with stochastic volatility. Journal of Business & Economic Statistics 29(3), 327–341.

Clark, T. E. and F. Ravazzolo (2015). Macroeconomic forecasting performance under alternative specifications of time-varying volatility. Journal of Applied Econometrics 30(4), 551–575.

D'Agostino, A., L. Gambetti, and D. Giannone (2013). Macroeconomic forecasting and structural change. Journal of Applied Econometrics 28(1), 82–101.

Dovern, J. and N. Jannsen (2017). Systematic errors in growth expectations over the business cycle. International Journal of Forecasting 33(4), 760–769.

Durbin, J. and S. J. Koopman (2001). Time Series Analysis by State Space Methods. Number 9780198523543 in OUP Catalogue. Oxford University Press.

Estrella, A. (2005). Why does the yield curve predict output and inflation? The Economic Journal 115(505), 722–744.

Estrella, A. and F. S. Mishkin (1997). The predictive power of the term structure of interest rates in Europe and the United States: Implications for the European Central Bank. European Economic Review 41(7), 1375–1401.

Evgenidis, A., S. Papadamou, and C. Siriopoulos (2020). The yield spread's ability to forecast economic activity: What have we learned after 30 years of studies? Journal of Business Research 106, 221–232.

Ferrara, L., M. Marcellino, and M. Mogliani (2015). Macroeconomic forecasting during the Great Recession: The return of non-linearity? International Journal of Forecasting 31(3), 664 – 679.

Foroni, C., P. Guérin, and M. Marcellino (2015). Markov-switching mixed-frequency VAR models. International Journal of Forecasting 31(3), 692–711.

Foroni, C. and M. Marcellino (2013). A survey of econometric methods for mixed-frequency data. Working Paper 2013/06, Norges Bank.

Garthwaite, P. H., Y. Fan, and S. A. Sisson (2016). Adaptive optimal scaling of metropolis–hastings algorithms using the robbins–monro process. Communications in Statistics-Theory and Methods 45(17), 5098–5111.

Geweke, J. (1993). Bayesian treatment of the independent student-t linear model. Journal of Applied Econometrics 8, S19–S40.

Gneiting, T. and R. Ranjan (2011). Comparing density forecasts using threshold and quantile weighted scoring rules. Journal of Business & Economic Statistics 29(3), 411–422.

Götz, T. B. and K. Hauzenberger (2018). Large mixed-frequency VARs with a parsimonious time-varying parameter structure. Discussion Papers 40/2018, Deutsche Bundesbank.

Heinrich, M. and M. Reif (2020). Real-Time Forecasting Using Mixed-Frequency VARs with Time-Varying Parameters. CESifo Working Paper Series 8054, CESifo Group Munich.

Jacquier, E., N. G. Polson, and P. E. Rossi (2002). Bayesian analysis of stochastic volatility models. Journal of Business & Economic Statistics 20(1), 69–87.

Jurado, K., S. C. Ludvigson, and S. Ng (2015). Measuring uncertainty. The American Economic Review 105(3), 1177–1216.

Karlsson, S. (2013). Forecasting with Bayesian vector autoregression. Handbook of Economic Forecasting 2, 791–897.

Kim, S., N. Shephard, and S. Chib (1998). Stochastic volatility: likelihood inference and comparison with ARCH models. The Review of Economic Studies 65(3), 361–393.

Koop, G. M. (2013). Forecasting with medium and large Bayesian VARs. Journal of Applied Econometrics 28(2), 177–203.

Korobilis, D. (2013). Hierarchical shrinkage priors for dynamic regressions with many predictors. International Journal of Forecasting 29(1), 43–59.

Litterman, R. B. (1986). Forecasting with Bayesian vector autoregressions – five years of experience. Journal of Business & Economic Statistics 4(1), 25–38.

Liu, W. and E. Moench (2016). What predicts US recessions? International Journal of Forecasting 32(4), 1138–1150.

Mariano, R. S. and Y. Murasawa (2003). A new coincident index of business cycles based on monthly and quarterly series. Journal of Applied Econometrics 18(4), 427–443.

Matheson, J. E. and R. L. Winkler (1976). Scoring rules for continuous probability distributions. Management Science 22(10), 1087–1096.

McCracken, M. W. and S. Ng (2016). FRED-MD: A monthly database for macroeconomic research. Journal of Business & Economic Statistics 34(4), 574–589.

Mumtaz, H. and P. Surico (2015). The transmission mechanism in good and bad times. International Economic Review 56(4), 1237–1260.

Mumtaz, H. and K. Theodoridis (2018). The changing transmission of uncertainty shocks in the US. Journal of Business & Economic Statistics 36(2), 239–252.

Pierdzioch, C. and R. Gupta (2019). Uncertainty and forecasts of US recessions. Studies in Nonlinear Dynamics & Econometrics Forthcoming.

Reif, M. (2020). Macroeconomic Uncertainty and Forecasting Macroeconomic Aggregates. Studies in Nonlinear Dynamics & Econometrics Forthcoming.

Schorfheide, F. and D. Song (2015). Real-Time forecasting with a mixed-frequency VAR. Journal of Business & Economic Statistics 33(3), 366–380.

Segnon, M., R. Gupta, S. Bekiros, and M. E. Wohar (2018). Forecasting US GNP growth: The role of uncertainty. Journal of Forecasting 37(5), 541–559.

Sinclair, T. M. (2019). Continuities and Discontinuities in Economic Forecasting. RPF Working Paper 2019-003, The George Washington University.

Tenreyro, S. and G. Thwaites (2016). Pushing on a string: US monetary policy is less powerful in recessions. American Economic Journal: Macroeconomics 8(4), 43–74.

Vrugt, J. A., C. Ter Braak, C. Diks, B. A. Robinson, J. M. Hyman, and D. Higdon (2009). Accelerating markov chain monte carlo simulation by differential evolution with self-adaptive randomized subspace sampling. International Journal of Nonlinear Sciences and Numerical Simulation 10(3), 273–290.

Wright, J. H. (2019). Some observations on forecasting and policy. International Journal of Forecasting 35(3), 1186 – 1192.

Appendix

A State-Space Representation

I follow Schorfheide and Song (2015) and split the state vector z_t from equation (1) such that it contains only the latent variable $z_t = z_{q,t} = [\tilde{y}'_{q,t}, \ldots, \tilde{y}'_{q,t-p}]'$ to decrease computation time. Let the remaining monthly variables be $z_{m,t-1} = [y'_{m,t-1}, \ldots, y'_{m,t-p}]'$. Hence, the measurement equation for the MF-T-CSVM-VAR can be written as:

$$y_t = C_{m,S_t} + R_{q,S_t} z_{q,t} + R_{m,S_t} z_{m,t-1} + B_{m,S_t} h_{t-1} + \Upsilon_{S_t} \tag{A.1}$$

where

$$\begin{aligned}
C_{m,S_t} &= \begin{bmatrix} 0_{nq,1} & A_{0m,S_t} \end{bmatrix}' \\
B_{m,S_t} &= \begin{bmatrix} 0_{nq,1} & b_{m,S_t} \end{bmatrix}' \\
R_{q,S_t} &= \begin{bmatrix} R_{q1,S_t} & R_{q2,S_t} \end{bmatrix}' \\
R_{q1,S_t} &= \begin{bmatrix} 1/3 * I_{nq} & 2/3 * I_{nq} & I_{nq} & 2/3 * I_{nq} & 1/3 * I_{nq} & 0_{nq \times nq * p} \end{bmatrix} \\
R_{q2,S_t} &= \begin{bmatrix} 0_{n-nq \times 1} & A_{mq,S_t} \end{bmatrix} \\
R_{m,S_t} &= \begin{bmatrix} R_{m1,S_t} & R_{m2,S_t} \end{bmatrix}' \\
R_{m1,S_t} &= \begin{bmatrix} 0_{nq \times nm*(p)} \end{bmatrix} \\
R_{m2,S_t} &= \begin{bmatrix} 0_{nq,nm*p} & A_{mm,S_t} \end{bmatrix}'.
\end{aligned}$$

with A_{0m,S_t} containing the intercepts for $y_{m,t}$, b_{m,S_t} being the parameters that relate $y_{m,t}$ to h_{t-1}, A_{mm,S_t} being a $(nm \times nm * p)$ matrix containing all VAR parameters that relates $y_{m,t}$ to $[y'_{m,t-1}, \ldots, y'_{m,t-p}]'$ and A_{mq,S_t} being a $(nm \times nq * p)$ matrix containing all VAR parameters that relates $y_{m,t}$ to $[\tilde{y}'_{q,t-1}, \ldots, \tilde{y}'_{q,t-p}]'$. The error term is divided into $\Upsilon_{S_t} = [0_{nq,1} u_{nm,t}]$. The transition equation is adjusted as follows:

$$z_{q,t} = C_{q,S_t} + A_{q,S_t} z_{q,t-1} + A_{m,S_t} z_{m,t-1} + B_{q,S_t} h_{t-1} + \upsilon_t \qquad \upsilon_t \sim \mathcal{N}(0, \Xi_{S_t}). \tag{A.2}$$

where

$$
\begin{aligned}
C_{q,S_t} &= \begin{bmatrix} A_{0q,S_t} & 0_{nq*p,1} \end{bmatrix}' \\
B_{q,S_t} &= \begin{bmatrix} b_{q,S_t} & 0_{nq*p,1} \end{bmatrix}' \\
A_{q,S_t} &= \begin{bmatrix} A_{qq,S_t} & I_{nq*p,nq*(p+1)} \end{bmatrix}' \\
A_{m,S_t} &= \begin{bmatrix} A_{qm,S_t} & 0_{nq*p,nm*(p+1)} \end{bmatrix}'.
\end{aligned}
$$

with A_{0q,S_t} containing the intercepts for $\tilde{y}_{q,t}$, b_{q,S_t} being the parameters that relate $\tilde{y}_{q,t}$ to h_{t-1}, A_{qq} being a $(nq \times nq*p)$ matrix containing all VAR parameters that relates $z_{q,t}$ to $z_{q,t-1}$ and A_{qm} being a $(nq \times nm*p)$ matrix containing all VAR parameters that relates $z_{q,t}$ to $z_{m,t-1}$.

B Prior

VAR-coefficients

I use an independent Normal-inverse-Wishart Minnesota prior for the VAR parameters. The prior mean on the first lag is 0 (0.9) if the respective variable is non-persistent (persistent) since all variables are transformed to be stationary. Thus, the prior mean for row j and column i of the coefficient matrix of lag l is set as follows:

$$
E(A_l^{j,i}) = \begin{cases} 0.9 & \text{if } i = j \text{ and } l = 1 \text{ and j is persistent} \\ 0 & \text{if } i = j \text{ and } l = 1 \text{ and j is non-persistent} \\ 0 & \text{otherwise.} \end{cases} \tag{A.3}
$$

The prior variance for row j and column i of the coefficient matrix of lag l is set as follows:

$$
Var(A_l^{j,i}) = \begin{cases} \frac{\lambda_1}{l^2} & \text{if } i = j \\ \frac{\lambda_1 \lambda_2 \sigma_{jj}^2}{l^2 \sigma_{ii}^2} & \text{if } i \neq j \\ \frac{\lambda_1 \lambda_3 \sigma_{jj}^2}{l^2 \sigma_{ii}^2} & \text{if } i \neq j \wedge j = y^* \\ 1000 & \text{if } l = 0 \end{cases} \tag{A.4}
$$

where σ_{ii} is the residual standard error of an AR(p) for variable i. The amount of shrinkage is determined by the vector of hyperparameters $\Lambda = [\lambda_1, \lambda_2, \lambda_3]'$. λ_1 governs the overall shrinkage. λ_2 applies cross-variable shrinkage and λ_3 as an extra shrinkage parameter for the business cycle variables, namely the business cycle index y^* (CFNAI) and the uncertainty factor h_t (CSVM). The prior variance for row j of the coefficient on h_{t-1} is $Var(b^{j,1}) = \frac{\lambda_1 \lambda_3 \sigma_{jj}^2}{\overline{\sigma^2}}$ where $\overline{\sigma^2}$ is the mean of the residual standard errors of AR(p) for each variable rescaled to have a variance of one. Starting values are $\Lambda = [0.04, 1, 1]'$ such that there is no cross-variable shrinkage and the overall shrinkage is in line with standard values picked for US data.

The prior scale matrix for the inverse-Wishart is diagonal:

$$p(\Omega) \sim \mathcal{IW}(S, \nu) \tag{A.5}$$

with $S = diag(\sigma_{11}^2, \ldots, \sigma_{NN}^2)$ where σ_{ii}^2 is again the residual variance of an AR(p) for variable i. The degrees of freedom ν are set to a minimum to account for a loose prior. The same prior is used across regimes $S_t = 1, 2$.

Shrinkage

I utilize a hyperprior to determine the degree of shrinkage in form of an inverse-Gamma prior:

$$p(\lambda_i) \sim \mathcal{IG}(\alpha, \beta_i) \qquad\qquad i = 1, 2, 3 \tag{A.6}$$

with shape $\alpha = 0.1$ and scale $\beta_i = 0.044$ for $i = 1, 2$ and scale $\beta_i = \sqrt{0.044}$ for $i = 3$ such that it is weakly informative and has a mode of 0.04 for $i = 1, 2$ which is in line with common values used for US data and with 0.2 for $i = 3$ giving a priori a less shrinkage for the business cycle variables assuming that those variables are more important.

Threshold Variable

I assume a uniform prior for the delay d and threshold parameter r:

$$d \sim \mathcal{U}(1, p) \tag{A.7}$$

$$r \sim \mathcal{U}(y_q^*, y_{1-q}^*). \tag{A.8}$$

where p is the maximum number of lags in the VAR and y_q^* denotes the qth quantile of the threshold variable. The quantile is set to 10% to avoid outlier regimes. Given the real-time information content regarding the NBER business cycle dating, recessions account for about 15% to 20% of observations such that 10% is a general reasonable lower bound.

The starting value for r is set according to a simple univariate threshold AR model with CFNAI. I apply the MCMC simulation by Vrugt et al. (2009) with $M = 10$ chains with 500000 draws based on 10 random starting values below the average $r < 0$. The posterior mean of the final chain provides a proper reasonable starting value for the more complex threshold VAR.

Common Stochastic Volatility

The CSV prior setting mainly follows Carriero et al. (2016). I initialize the factor f_t with a Normal prior:

$$f_t \sim \mathcal{N}(1, 0.5) \tag{A.9}$$

and the variance of the innovations of the random walk law of motion by an inverse-Gamma distribution:

$$\phi \sim \mathcal{IG}(4, 0.04) \tag{A.10}$$

Furthermore, $f_t\Sigma$ is identified up to scale. Hence, I fix $f_0 = 1$ for indentification.

Latent state

I follow Schorfheide and Song (2015) for the prior on the latent state variable $z_{q,t}$ and initialize the Kalman filter with a Normal prior:

$$p(z_{q,0}) \sim N(z_{q,-1}, I). \tag{A.11}$$

where I use a training sample of one year to estimate $z_{q,-1}$ with a linear MF-VAR based on actual observations for the monthly variables, interpolated values for the quarterly latent values and VAR parameters resting on their prior means.

C Metropolis-within-Gibbs sampler

In the following I explain in detail each step of the MCMC algorithm for the MF-T-CSVM-VAR since all other models can be estimated by skipping the respective step in the sampler and in the conditioning set. I employ a total of 30000 iterations where the first 25000 are used as burn-in draws. A vector of variables over time T is denoted by $x^T = [x_1', \dots, x_T']'$. For the remainder A_{S_t} indicates the coefficient matrix of all VAR(p) dynamics including A_{0,S_t} and b_{1,S_t} for $S_t = 1, 2$ as it is estimated in the same step. The sequence for the MCMC is as follows:

1. Initialize A_1, Λ_1, Σ_1, A_2, Λ_2, Σ_2 , r, d, ϕ, f^T
2. $p(\tilde{y}^T | A_1, \Lambda_1, \Sigma_1, A_2, \Lambda_2, \Sigma_2, r, d, \phi, f^T, y^T)$
3. $p(A_1 | \tilde{y}^T, \Lambda_1, \Sigma_1, A_2, \Lambda_2, \Sigma_2, r, d, \phi, f^T)$
4. $p(\Sigma_1 | \tilde{y}^T, A_1, \Lambda_1, A_2, \Lambda_2, \Sigma_2, r, d, \phi, f^T)$
5. $p(A_2 | \tilde{y}^T, A_1, \Lambda_1, \Sigma_1, \Lambda_2, \Sigma_2, r, d, \phi, f^T)$
6. $p(\Sigma_2 | \tilde{y}^T, A_1, \Lambda_1, \Sigma_1, A_2, \Lambda_2, r, d, \phi, f^T)$
7. $p(\Lambda_1 | \tilde{y}^T, A_1, \Sigma_1, A_2, \Lambda_2, \Sigma_2, r, d, \phi, f^T)$
8. $p(\Lambda_2 | \tilde{y}^T, A_1, \Lambda_1, A_2, \Sigma_1, \Sigma_2, r, d, \phi, f^T)$
9. $p(r | \tilde{y}^T, A_1, \Lambda_1, \Sigma_1, A_2, \Lambda_2, \Sigma_2, d, \phi, f^T)$
10. $p(d | \tilde{y}^T, A_1, \Lambda_1, \Sigma_1, A_2, \Lambda_2, \Sigma_2, r, \phi, f^T)$
11. $p(\phi | \tilde{y}^T, A_1, \Lambda_1, \Sigma_1, A_2, \Lambda_2, \Sigma_2, r, d, f^T)$
12. $p(f^T | \tilde{y}^T, A_1, \Lambda_1, \Sigma_1, A_2, \Lambda_2, \Sigma_2, r, d, \phi)$

After step 2., one can drop the conditioning on the data y^T since the data does not provide any further information after condition on the latent state $\tilde{y}^T$. Conditional on r, d and $\tilde{y}^T$, the sample is split into two regimes $S_t = 1, 2$. Furthermore, conditional on f^T, one can transform

$\check{y}^T = \frac{1}{\sqrt{f^T}}\tilde{y}^T$. Hence, step 3.-6. are standard draws from the multivariate Normal distribution for $p(A_{S_t}|\cdot)$ and from the inverse-Wishart for $p(\Sigma_{S_t}|\cdot)$ based on the subsamples and transformed variables $\check{y}^T$. Drawing the variance ϕ of log-volatilities is, conditional on f_t, from an inverse-Gamma distribution.

The Gibbs sampler includes two Metropolis-Hastings step. Step 9. uses a random walk for the threshold r and step 12. an independence chain Metropolis-Hastings for the stochastic volatility f_t. Apart from the standard draws, the remaining steps draw from the following conditional posterior distributions:

2. Step: Latent states $z_{q,t}$ to obtain $\tilde{y}_{q,t}$:
   Draws for $z_{q,t}$ are based on the algorithm by Carter and Kohn (1994). To this end, I apply the Kalman filter until T to estimate the mean $z_{q,T|T}$ as well as the covariance matrix $P_{T|T}$. Hence, I draw $z_{q,T}$ from $N(z_{q,T|T}, P_{T|T})$. After backward smoothing the state vector recursively for $t = T-1, \ldots, 1$, I draw $z_{q,t}$ from $N(z_{q,t|t}, P_{t|t})$

7. and 8. Step: Shrinkage parameters Λ_{S_t}:
   To simplify notation, I drop the index S_t. Conditional on all other parameters, $\Lambda = [\lambda_1, \lambda_2, \lambda_3]'$ only affects the VAR coefficients through its prior dependence. Since the prior variance $Var(A) = \underline{V}$ is diagonal, one can operate row-wise by selecting the respective elements containing λ_i from the prior variance. Hence, the conditional posterior simplifies to:

$$p(\lambda_i|\lambda_{-i}, \tilde{y}^T, A, \Sigma, r, d, \phi, f^T) \propto p(A_i|\lambda_i)p(\lambda_i) \qquad \forall\, i = 1, 2, 3 \tag{A.12}$$

   where $p(A_i|\lambda_i)$ denotes prior distribution of all elements of A associated with λ_i and $p(\lambda_i)$ indicates the prior distribution for the hyperparameter. λ_{-i} are the remainder shrinkage parameters excluding i. The conditional posterior $p(\lambda_i|\ldots) \sim \mathcal{IG}(\overline{a}, \overline{b})$ is inverse-Gamma with posterior shape and scale:

$$\overline{a} = \underline{a} + 1/2 * k_i \tag{A.13}$$

$$\overline{b} = 1/2 * \left((vec(A_i) - vec(\underline{A}_i))'\underline{V}^{-1}(vec(A_i) - vec(\underline{A}_i)) + \underline{b}\right) \tag{A.14}$$

   where k_i refers to the number of parameters attached to λ_i, $\underline{a}$ and $\underline{b}$ indicate prior shape and scale and $vec()$ is the vectorization operator. $\underline{A}_i$ denotes the prior mean of A_i.

9. Step: Threshold value r:
   The conditional posterior distribution of r is analytical infeasible given by:

$$p(r|\cdot) = |\Sigma|_1^{T_1}|\Sigma|_2^{T_2} exp\left(-\sum_{S_t=1}^{2}(\check{Y}_{S_t} - \check{X}_{S_t}A_{S_t})'\Sigma_{S_t}^{-1}(\check{Y}_{S_t} - \check{X}_{S_t}A_{S_t})\right) \tag{A.15}$$

where T_1 and T_2 are the sample size of regime 1 and 2, respectively. Since the prior for r is uniform, the acceptance probability for the Metropolis-Hastings step at iteration s is

$$\alpha_r^s = min\left(\frac{p(r^*|\cdot)}{p(r^{s-1}|\cdot)}, 1\right) \quad \text{for } S_t = 1, 2 \tag{A.16}$$

where the proposal r^* is generated by a random walk:

$$r^* = r^{s-1} + \vartheta \qquad \vartheta \sim N(0, \sigma_r^2). \tag{A.17}$$

The standard deviation σ_r is adjusted in iteration s according to the method proposed by Garthwaite et al. (2016):

$$\sigma_r^s = \sigma_r^{s-1} + c(\alpha^{s-1} - \alpha^*)/(s-1), \tag{A.18}$$

where $\alpha^* = 0.4$ is the target acceptance rate and $c = 1/[\alpha^*(1-\alpha^*)]$ is the optimal step size.

10. Step: Delay parameter d:

    The conditional posterior distribution $p(d|\cdot)$ is a multinomial distribution:

$$p(d|\cdot) = \frac{L(A_1, A_2, \Sigma_1, \Sigma_2, r, d|\check{y}^T)}{\sum_{d=1}^{p} L(A_1, A_2, \Sigma_1, \Sigma_2, r, d|\check{y}^T)} \tag{A.19}$$

    where $L(\cdot|\check{y}^T)$ denotes the likelihood function conditional on the transformed latent state $\check{y}^T$ and $\sum_{d=1}^{p}$ adds up all likelihoods based on the support of the uniform prior $d \sim \mathcal{U}(1, p)$ with p being the lag order of the VAR.

12. Step: Stochastic volatility f_t:

    The draw is based on the algorithm by Jacquier et al. (2002). For each draw of f_t, given the random walk law of motion, only the knowledge of f_{t+1} and f_{t-1} is relevant:

$$p(f_t|f_{-t}, \ldots) = p(f_t|f_{t-1}, f_{t+1}, \ldots) \tag{A.20}$$

    such that the conditional posterior is the product of a Normal density arising from the likelihood and a log-Normal density arising from the random walk law of motion of $h_t = ln(f_t)$. A log-Normal density is taken as a proposal and then progresses for $t = 1, \ldots, T$ cycling through T Metropolis-Hastings steps. I refer to Jacquier et al. (2002) for more details. One simply needs to adjust for the exact likelihood of the VAR model and the exact law of motion for the for stochastic volatility in case-by-case.

D Forecast - Additional Figures

Figure 6: Monthly GDP from the MF-T-CSVM-VAR

(a) in monthly growth rates

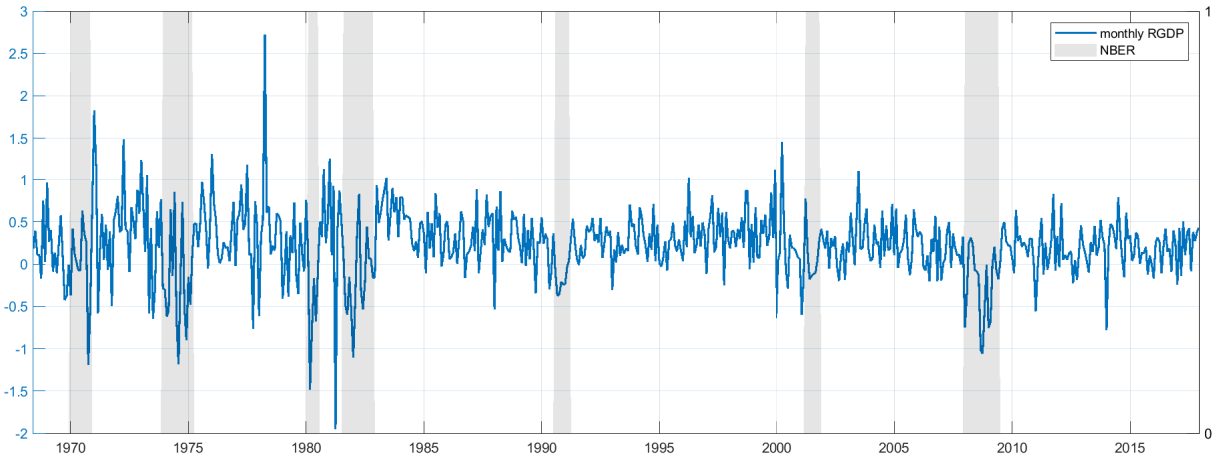

(b) in quarterly growth rates

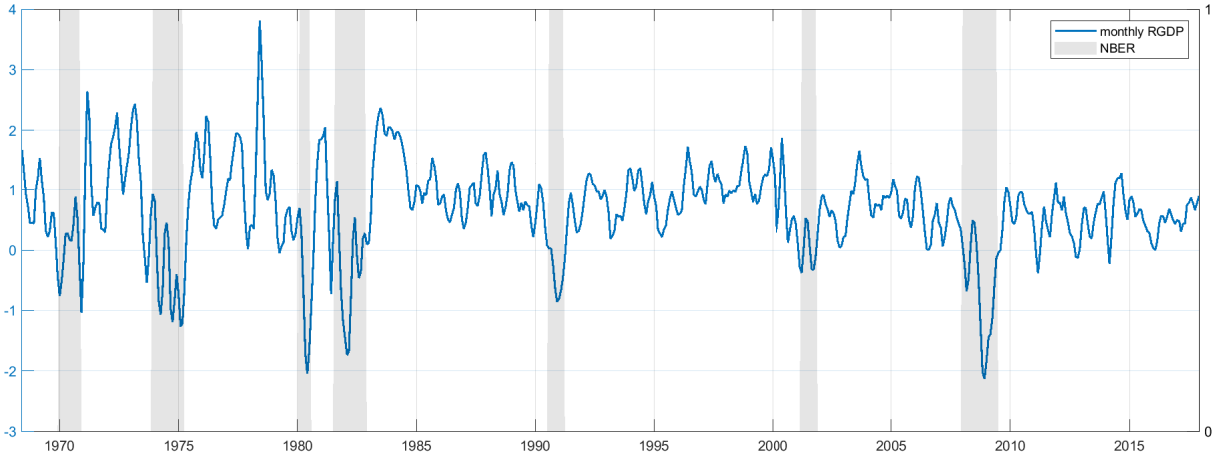

Notes: Panel (a) corresponds to $\tilde{y}_{q,t}$ from equation (3). Panel (b) corresponds to $y_{q,t}$ from equation (3). Shaded areas correspond to the recessions dated by the NBER. Sample: 1967M4-2017M12

Figure 7: RMSE relative to SPF - GDP

(a) Full sample

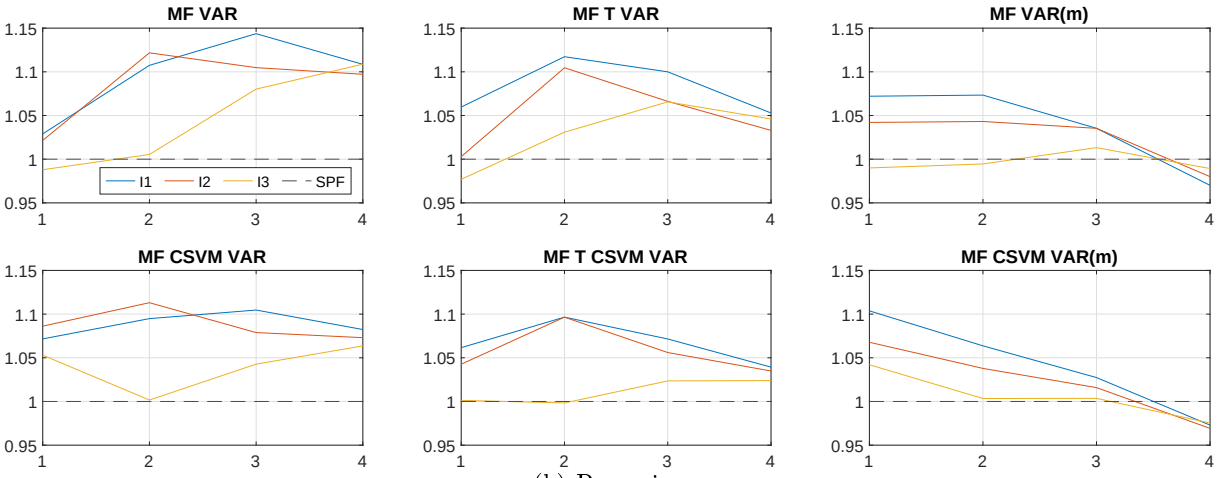

(b) Recession

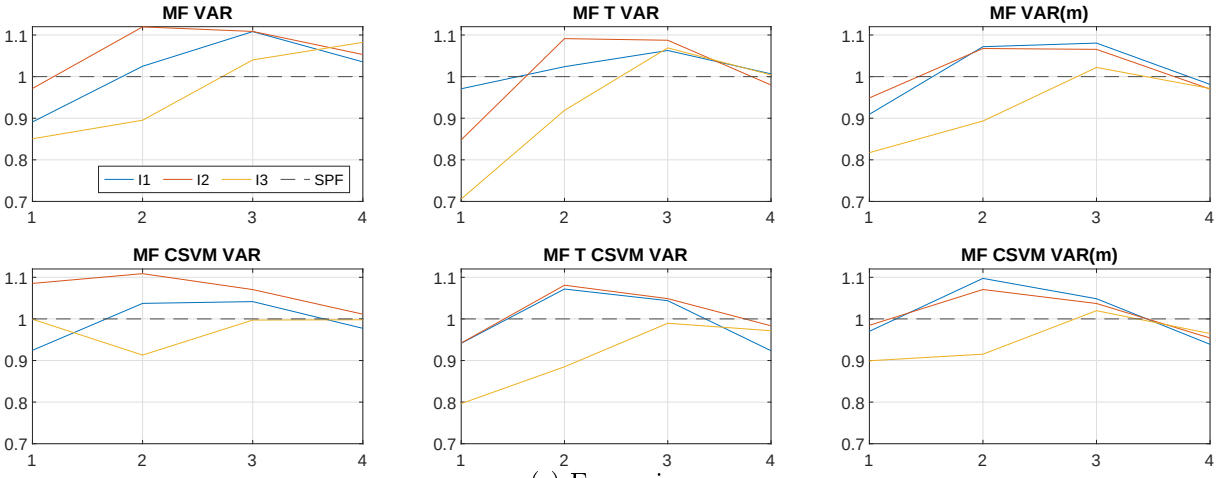

(c) Expansion

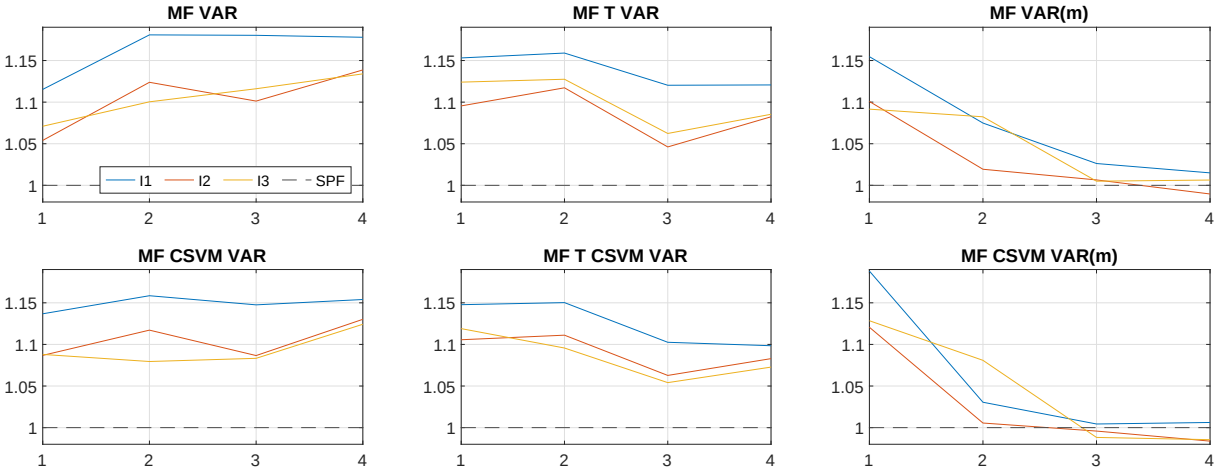

Notes: The relative RMSEs are expressed as ratios relative to the SPF for horizons $h = 1, \ldots, 4$. A figure below unity indicates that the model outperforms the SPF. The blue, red and yellow line belong to information set I1, I2 and I3, respectively, as explained in Section 4.5. Figure (a) refers to the full sample. Figure (b) and (c) refer to the NBER recession and expansion subsample, respectively. Out-of-sample: 2001M2-2017M12

Figure 8: RMSE relative to SPF - UR

(a) Full sample

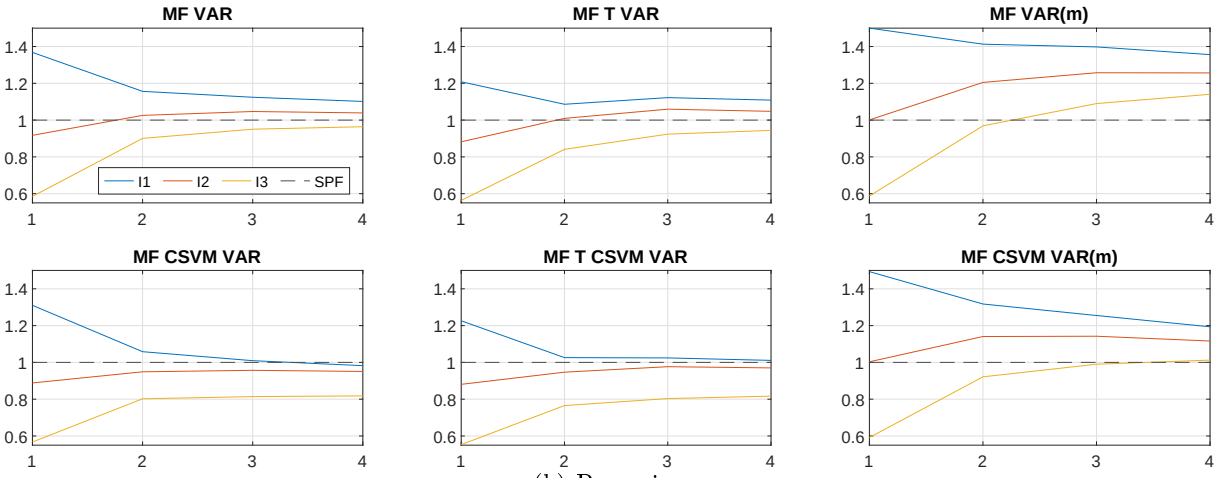

(b) Recession

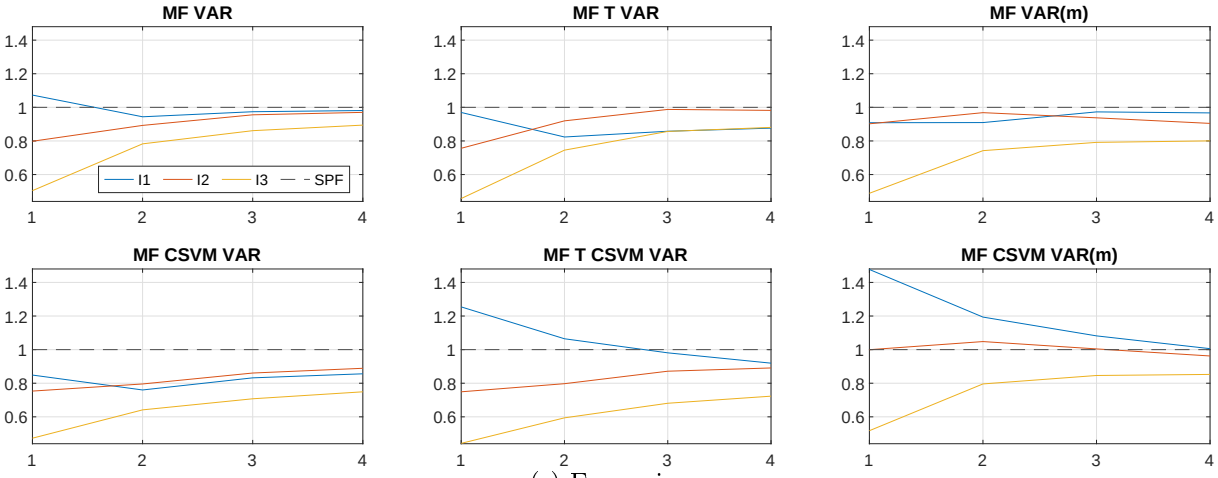

(c) Expansion

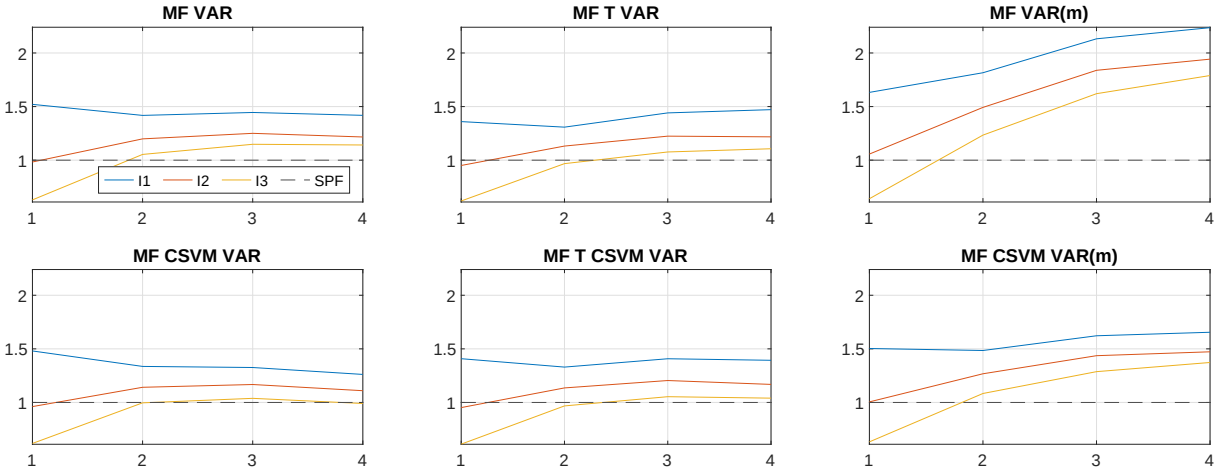

Notes: The relative RMSEs are expressed as ratios relative to the SPF for horizons $h = 1, \ldots, 4$. A figure below unity indicates that the model outperforms the SPF. The blue, red and yellow line belong to information set I1, I2 and I3, respectively, as explained in Section 4.5. Figure (a) refers to the full sample. Figure (b) and (c) refer to the NBER recession and expansion subsample, respectively. Out-of-sample: 2001M2-2017M12.

E Shrinkage and Forecasting

Each model that contains either the CFNAI business cycle index and/or the CSVM uncertainty factor have an separate cross variable shrinkage parameter λ_3 such that those variables might get less shrinkage due to their importance for forecasting. However, the standard Minnesota prior usually comes with a single cross variable shrinkage parameter ($\lambda_3 = \lambda_2$). Hence, I compare those two shrinkage setups with respect to their point forecast accuracy. Figure 9 displays a heatmap based on the relative RMSEs. The relative RMSEs are expressed as ratios relative to the same model with cross variable shrinkage. A figure below unity indicates that the model with BC shrinkage ($\lambda_3 \neq \lambda_2$) performs better.

The first detail one notice is that RMSEs are significantly reduced for GDP and UR during recessions for both T-VARs. While this is noticeable for GDP only for h=1, it is significantly better for UR across all forecast horizons. However, also for UR the improvements are strongest with up to 11% in relative RMSEs for the MF-T-CSVM-VAR for h=1. This advantage is no longer present in expansion in any way. Neither the small-scale nor the medium-scale VARs can improve their RMSEs by BC shrinkage during expansions.

In summary, the influence of the BC shrinkage on forecasting accuracy is stronger in times of recessions than expansions. Whereby the advantages in recession outweigh the slight disadvantages in expansion for the full sample. That means less shrinkage for CFNAI and CSVM is beneficial during recessions emphasizing the important information for short term forecasting contained in both BC variables during deteriorating times.

Figure 9: Relative RMSEs - BC Shrinkage against Cross Variable Shrinkage

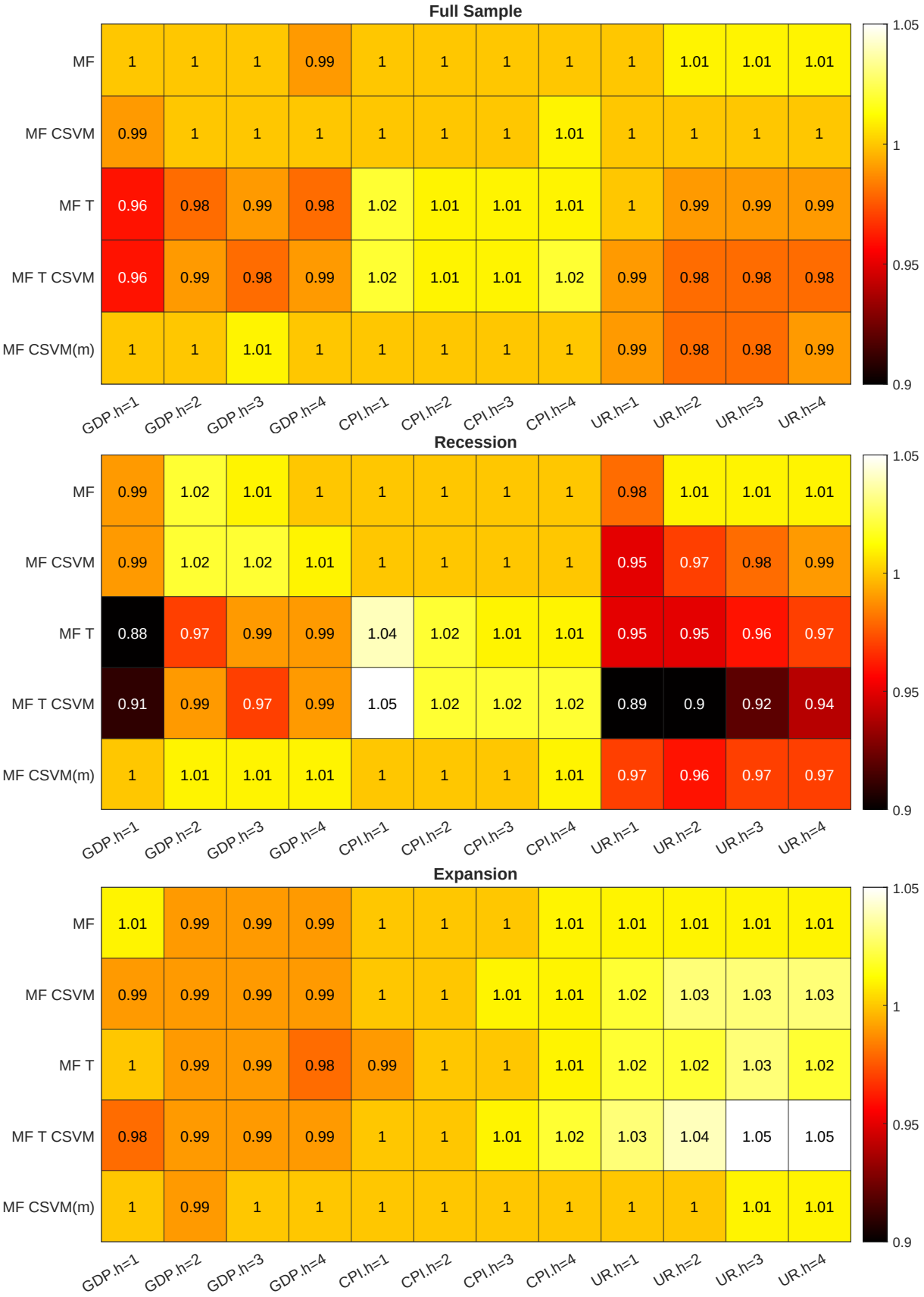

Notes: The relative RMSEs are expressed as ratios relative to the same model with cross variable shrinkage ($\lambda_3 = \lambda_2$). A figure below unity indicates that the model with BC shrinkage ($\lambda_3 \neq \lambda_2$) performs better. Hence, a panel with a darker shade corresponds to an increase in forecast accuracy. MF-VAR^{med} and MF-VAR^{b} are left out since the do not include λ_3. The upper, middle and lower panel belong to the full sample, the recession subsample and expansion subsample, respectively. Out-of-sample: 2001M2-2017M12.

F Real-Time Data Set

Name	Transformation	ALFRED Code
Real Gross Domestic Product (GDP)	1	GDPC1
Consumer Price Index for All Urban Consumers: All Items (CPI)	1	CPIAUCSL
Civilian Unemployment Rate	4	UNRATE
All Employees: Total Nonfarm Payrolls	1	PAYEMS
Yield Spread (YS), 10-year - 3-month treasury bill rate	4	GS10-TB3MS
S&P 500 Index	1	(FRED-MD)
Chicago Fed National Activity Index	4	(Chicago Fed)
Industrial Production Index	1	INDPRO
Capacity Utilization: Total Industry	2	TCU
Housing Starts: Total	3	HOUST
Real Personal Consumption Expenditures	1	PCEC96
Index of Aggregate Weekly Hours	2	AWHI
Real Manufacturing and Trade Sales	1	(FRED-MD)
New Orders Durable Goods	1	(FRED-MD)

Transformation: 1. $\Delta ln(y_t)$ 2. Δy_t 3. $ln(y_t)$ 4. y_t. Additional Sources: Chicago Fed https://www.chicagofed.org/publications/cfnai/index. FRED-MD https://research.stlouisfed.org/econ/mccracken/fred-databases/.